NRC Research Press

ARTICLE

Using species distribution models to describe essential fish habitat in Alaska

Edward A. Laman, Christopher N. Rooper, Kali Turner, Sean Rooney, Dan W. Cooper, and Mark Zimmermann

Abstract: Describing essential habitat is an important step toward understanding and conserving harvested species in ecosystem-based fishery management. Using data from fishery-independent ichthyoplankton, groundfish surveys, and commercial fisheries observer data, we utilized species distribution modeling techniques to predict habitat-based spatial distributions of federally managed species in Alaska. The distribution and abundance maps were used to refine existing essential fish habitat descriptions for the region. In particular, we used maximum entropy and generalized additive modeling to delineate distribution and abundance of early (egg, larval, and pelagic juvenile) and later (settled juvenile and adult) life history stages of groundfishes and crabs across multiple seasons in three large marine ecosystems (Gulf of Alaska, eastern Bering Sea, and Aleutian Islands) and the northern Bering Sea. We present a case study, featuring Kamchatka flounder (*Atheresthes evermanni*), from the eastern and northern Bering Sea to represent the >400 habitat-based distribution maps generated for more than 80 unique species–region–season–life-stage combinations. The results of these studies will be used to redescribe essential habitat of federally managed fishes and crabs in Alaska.

Résumé : La description des habitats essentiels est une étape importante pour la compréhension et la conservation des espèces exploitées dans une approche écosystémique de gestion des pêches. En utilisant des données indépendantes de la pêche sur l'ichtyoplancton, des données de campagnes d'évaluation des poissons de fond et des données d'observateurs sur les pêches commerciales, nous avons employé des techniques de modélisation de la répartition des espèces pour prédire les répartitions spatiales basées sur l'habitat d'espèces faisant l'objet d'une gestion fédérale en Alaska. Les cartes de répartition et d'abondance ont été utilisées pour raffiner les descriptions existantes des habitats essentiels de poissons pour la région. En particulier, nous avons utilisé l'entropie maximum et la modélisation additive généralisée pour délimiter la répartition et l'abondance des stades précoces (œuf, larve et juvénile pélagique) et plus tardifs (juvénile établi et adulte) de poissons de fond et de crabes sur plusieurs saisons dans trois grands écosystèmes marins (golfe de l'Alaska, mer de Behring orientale et Aléoutiennes) et dans la mer de Behring septentrionale. Nous présentons une étude de cas, sur le flétan du Pacifique (*Atheresthes evermanni*), de la mer de Behring orientale et septentrionale pour représenter les plus de 400 cartes de répartition basée sur l'habitat générées pour plus de 80 combinaisons uniques d'espèce, de région, de saison et de stade du cycle de vie. Les résultats de ces études seront utilisés pour produire de nouvelles descriptions des habitats essentiels des poissons et crabes faisant l'objet d'une gestion fédérale en Alaska. [Traduit par la Rédaction]

Introduction

Countries around the world have begun integrating the concepts of ecosystem-based fisheries management (EBFM) into their resource management strategies (e.g., Shelton 2007; Metcalf et al. 2009; Hegland et al. 2015). Traditional fisheries management focuses on single species assessment, whereas EBFM breaks with this tradition to holistically address the ecosystem as a management priority (Pikitch et al. 2004). A fundamental component of the shift toward EBFM is considering habitats that are critical to species for vital processes such as feeding, growth, and reproduction in management strategies. Awareness of the importance of conserving critical habitats as a basic step in EBFM is recognized around the world (e.g., Hernandez-Delgado and Sabat 2000 in Puerto Rico; Stal et al. 2007 in Sweden) and has been formalized by the inclusion of essential fish habitat (EFH) provisions in the regulatory structure of fisheries management in the US and other regions (Rosenberg et al. 2000).

In the US exclusive economic zone, the re-authorization of the Magnuson–Stevens Fishery Conservation and Management Act (1996), hereinafter referred to as "the Act", mandates that the National Marine Fisheries Service (NMFS) identify EFH of managed species and act to conserve those habitats from adverse effects using the best scientific information available. EFHs are defined as the waters and substrata "necessary to fish for spawning, breeding, feeding or growth to maturity" (NMFS 2010) and compliments the EBFM concept of understanding which habitat is critical to species for vital processes. The North Pacific Fishery Management Council (NPFMC), which develops fishery management plans (FMPs) in Alaska, is required by the Act to consult with NMFS when their FMPs impinge on EFH. In this way, their management efforts can be designed to minimize the adverse effects of human activities on EFH while identifying actions that encourage its conservation and enhancement. An executive order issued in 2010 (Executive Order 13547; Federal Register 2010) has further emphasized this approach by establishing a national policy that prioritizes an ecosystem-based approach as the ruling principle guiding comprehensive management of aquatic resources. Finally, the Act mandates that all EFH provisions and information be periodically

Received 5 May 2017. Accepted 22 September 2017.

E.A. Laman, C.N. Rooper, K. Turner, S. Rooney, D.W. Cooper, and M. Zimmermann. National Marine Fisheries Service, Alaska Fisheries Science Center, 7600 Sand Point Way, NE, Seattle, WA 98115, USA.

Corresponding author: Edward A. Laman (email: Ned.Laman@NOAA.gov).

reviewed with the intent to improve the underlying science and add new data where appropriate. The present work helped NMFS meet the requirement of completing this periodic review.

The details of the types of information necessary to meet the Act's requirements for describing EFH of federally managed species are formalized in the Essential Fish Habitat Final Rule 50 (2002). They are grouped into four categorical levels based on the quality and types of data available (EFH Level 1: distribution data (presence–absence); EFH Level 2: habitat-specific densities; EFH Level 3: habitat-specific growth, reproduction, or survival rates; and EFH Level 4: habitat-specific production rates). Until our work was completed, all EFH descriptions for federally managed species in Alaska had been categorized using Level 1 information (distribution data only) or remained undescribed (Sigler et al. 2012). These EFH descriptions, derived from research survey and commercial catch distribution data, delineate areas intended to circumscribe 95% of a species' population.

Species distribution models (SDMs) have been used in conservation biology to describe the distribution and potential habitat of organisms in both marine and terrestrial systems (e.g., Kumar and Stohlgren 2009; Moore et al. 2009; Sheehan et al. 2017). We chose this approach to redescribe EFH in Alaska because it allowed us to identify important habitat covariates for delineating the spatial extent of a species' distribution. Additionally, this modeling technique provides us with a tool that outlines species–environment relationships on scales that are meaningful in marine spatial planning. Elith and Leathwick (2009) indicated that the usefulness of SDMs in ecosystem-based management will depend on the inclusion of functionally relevant covariates in the model formulations. Furthermore, the extent and boundaries of large marine ecosystems (LMEs), like the eastern Bering Sea, depend on the linked ecological criteria of bathymetry, hydrography, productivity, and trophic relationships. We chose habitat covariates to include in our SDM formulations that describe these four criteria and represent a variety of processes and habitat factors with the potential to affect the distribution of fish life stages (e.g., primary productivity, ocean currents, biogenic structures, water temperature). We applied SDM techniques to the early life history stages (ELHS) of fishes (i.e., egg, larval, and pelagic juvenile) as well as to later life stages of fishes and invertebrates (i.e., settled juveniles and adults) from the eastern and northern Bering Sea using independent, habitat-based covariates to predict their distributions and abundance.

The work presented here focuses on the early and later life history stages of Kamchatka flounder (*Atheresthes evermanni*) in the eastern and northern Bering Sea and demonstrates the first application of SDM technique to describe essential habitat for marine spatial planning in Alaska. This case study was part of a larger project, the goal of which was to describe EFH for all federally managed marine species in Alaska. The study objectives were (*i*) to redescribe EFH for federally managed species in Alaska using SDMs and (*ii*) to increase the level of information used to describe and identify EFH for strategic marine resource management. The resulting habitat-based distribution maps will refine descriptions of EFH for species found in the region and provide insight into the marine systems where these species occur. New descriptions of EFH for federal management plans in Alaska were recently completed for the eastern Bering Sea LME and northern Bering Sea (Laman et al. 2017) and the Aleutian Islands LME (Turner et al. 2017); new descriptions for the Gulf of Alaska LME are nearly complete (S. Rooney, E.A. Laman, C.N. Rooper, K. Turner, D.W. Cooper, and M. Zimmermann, unpublished data).

Materials and methods

Survey area

The eastern Bering Sea shelf, eastern Bering Sea upper continental slope, and the northern Bering Sea comprise the study area selected to demonstrate the SDM techniques used to redescribe EFH. Hereinafter, we will collectively refer to this study area as the eastern Bering Sea, which encompasses a diverse mosaic of benthic habitats that extend northward from the Aleutian Islands, Alaska Peninsula, and Bristol Bay to the Bering Strait in the north, is bordered in the northwest by the US–Russia Convention Line, in the west by the upper continental slope, and to the east by Norton Sound and the western shore of North America (Fig. 1). Much of the shelf is shallow and flat, extending more than 200 km from shore, generally at depths >100 m. The seafloor of the eastern Bering Sea shelf is composed mostly of soft unconsolidated sediments (Smith and McConnaughey 1999; Rooper et al. 2016). The eastern Bering Sea upper continental shelf slope (~200 m to 1000 m) is steep and includes five major canyon systems along its north–south extent. The seafloor of the eastern Bering Sea upper continental slope is more diverse than that on the shelf, with areas of rocky substrata, especially in Pribilof Canyon. Similar to the shelf, however, much of the continental slope is dominated by soft, unconsolidated sediments (Rooper et al. 2016). The northern Bering Sea is considered a distinct region from and is not as well described as the more frequently sampled eastern Bering Sea shelf and slope. Grebmeier et al. (1988) indicated that the seafloor in the northern Bering Sea near Norton Sound is shallow with mean water depths <50 m and is made up of unconsolidated sediments similar to those found on the eastern Bering Sea shelf. The eastern Bering Sea shelf is commonly divided into three domains based on bathymetry and oceanographic fronts: the inner shelf (0 to 50 m), middle shelf (50 to 100 m), and outer shelf (100 to 180 m; Coachman 1986). The shelf break is typically at 180 to 200 m depth, except at the northern edge of Bering Canyon, where the shelf break is at 500 m (Sigler et al. 2015).

Dependent variables: fish and invertebrate data

We used three sources of survey data from the eastern Bering Sea in our SDMs, each differing in terms of spatiotemporal coverage and sampling design (Fig. 2). Presence data for ELHS were provided from numerous Ecosystems and Fisheries-Oceanography Coordinated Investigations (EcoFOCI) ichthyoplankton surveys targeting different species, life stages, and seasons. Presence of *Atheresthes* spp. ELHS in the water column delineated what we termed the "oceanographic season" for this species. Summer distributions of settled juveniles and adults were modeled from the systematic Alaska Fisheries Science Center Resource Assessment and Conservation Engineering – Groundfish Assessment Program (RACE-GAP) summer bottom trawl surveys of the eastern Bering Sea shelf (Lauth and Conner 2014), eastern Bering Sea upper continental slope (Hoff 2013), and the northern Bering Sea (Lauth 2011). The third source of data used to model species distributions was collected by NMFS observers aboard commercial fishing vessels. These presence observations were integrated with vessel movement data acquired by satellite through the Vessel Monitoring System (VMS) and recorded in the VMS–Observer Enabled Catch-in-Areas database (VOE-CIA), which was supplied to us by the Alaska Regional Office (AKRO). Fishery-dependent commercial observer VOE-CIA data from fall (October–November), winter (December–February), and spring (March–May) comprised the third source of data in our analyses.

Historical ichthyoplankton catches from EcoFOCI's ichthyoplankton surveys of the eastern Bering Sea (1991–2013) were collected throughout the study area on a variety of surveys occurring at different times of the year and with differing objectives, target depths, and gear types (Matarese et al. 2003). Since the survey platforms, objectives, and gear types varied, ELHS of the fishes collected by EcoFOCI were included as presence-only data. Ichthyoplankton samples were combined across all available years for analysis. The spatial coverage of these data was also not uniform, with most samples coming from the southwestern portion of the eastern Bering Sea shelf. Kamchatka flounder eggs, larvae,

Fig. 1. Eastern Bering Sea from the Alaska Peninsula to the northern Bering Sea where this modeling study was carried out. Dots indicate the locations of bottom trawl hauls from the eastern Bering Sea shelf annual bottom trawl survey (1982–2014), the eastern Bering Sea slope biennial bottom trawl survey (2002–2012), and the northern Bering Sea survey (2010).

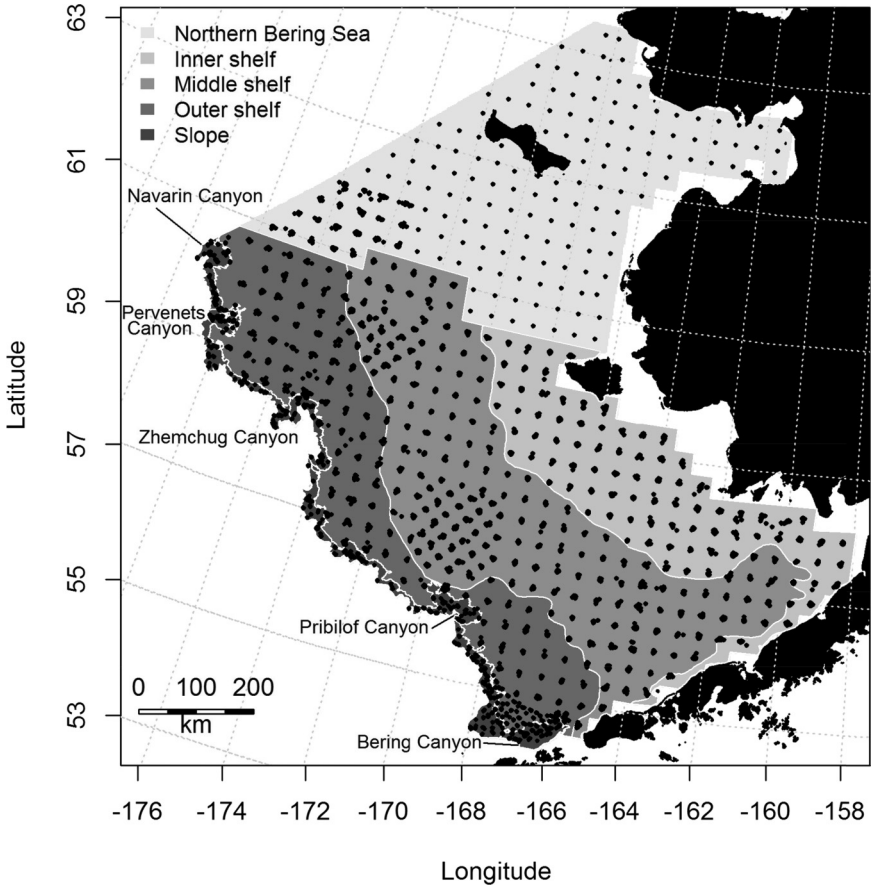

and pelagic juveniles have not historically been visually distinguished from those of its co-occurring close congener, arrowtooth flounder (*Atheresthes stomias*), in EcoFOCI ichthyoplankton samples (Matarese et al. 2003; De Forest et al. 2014). The early life stages of both species were collected together in ichthyoplankton surveys of the eastern Bering Sea (IIS 2016) and, consequently, ELHS SDMs were formulated for the generic *Atheresthes* spp. group as a proxy for Kamchatka flounder ELHS.

Scientific bottom trawl survey samples have been collected in the eastern Bering Sea since the 1940s, but the first systematic survey of the eastern Bering Sea shelf was conducted in 1975 by the US Bureau of Land Management (Lauth and Conner 2014). The RACE-GAP eastern Bering Sea shelf summer bottom trawl survey data has been collected from a regular 25 nautical mile (1 n.m. = 1.852 km) grid continuously since 1982. In recent years, this grid has been extended to include the northern Bering Sea and Norton Sound (Lauth 2011). Additionally, a bottom trawl survey of the eastern Bering Sea slope has been conducted quasibiennially during even-numbered years since 2000 over the upper continental shelf and slope at depths from 200 to 1200 m (Hoff and Britt 2011). The slope survey randomly samples existing stations within depth and area strata, with the addition of new stations each year. We combined the eastern Bering Sea shelf and slope with the northern Bering Sea survey stations (12 702 stations total) across years since 1982 for inclusion in our SDMs. Although the eastern Bering Sea bottom trawl survey methodology has been standardized since 1982 (Lauth and Conner 2014), Kamchatka flounder were not consistently separated from its close congener, arrowtooth flounder, in RACE-GAP summer bottom trawl catches until after 1992, effectively reducing the data set for our case study to the survey years 1993–2014.

Bottom trawl catches of Kamchatka flounder from RACE-GAP summer surveys were converted to swept-area estimates of catch-per-unit-effort (CPUE; Alverson and Pereyra 1969; Wakabayashi et al. 1985); length composition of the catch was also determined. For the dependent variable in SDM formulations, we used either Kamchatka flounder CPUE (number·ha^{-1}) or binary presence–absence. The approximate length at first maturity of female Kamchatka flounder (520 mm; Stark 2012) was used to distinguish between settled juveniles (≤520 mm fork length (FL)) and adults (>520 mm FL) in the length subsample. The proportional contribution of these two life stages to the random subsample of lengths from that catch was then used to apportion trawl-haul-specific Kamchatka flounder CPUE into settled juveniles and adults.

The third source of dependent data used in the SDMs was presence data from the VOE-CIA database populated with data collected by NMFS observers aboard commercial fishing vessels. Observed catches were combined across the years 2003–2013 and were used in our analyses. Fisheries under observation (e.g., walleye pollock (*Gadus chalcogrammus*) or yellowfin sole (*Limanda aspera*)) and the fishing gears they deployed were not distinguished, and all Kamchatka flounder presence observations were combined. Only the fall, winter, and spring seasons were considered for analyses because the summer distributions were modeled using RACE-GAP bottom trawl survey data.

Independent covariates: habitat data

The independent covariates used to parameterize and then select the best-fitting SDMs were chosen from a suite of habitat

Fig. 2. Density plots of the distribution of unique data points used to model the distribution of early and later life stages of fishes and invertebrates in the eastern and northern Bering Sea from ichthyoplankton (EcoFOCI data), bottom trawl surveys (summer), and observer data (fall, winter, and spring); data were aggregated on a 25 km × 25 km grid and scaled to the maximum value in a grid cell (blank areas (white space) indicate locations where no data were collected).

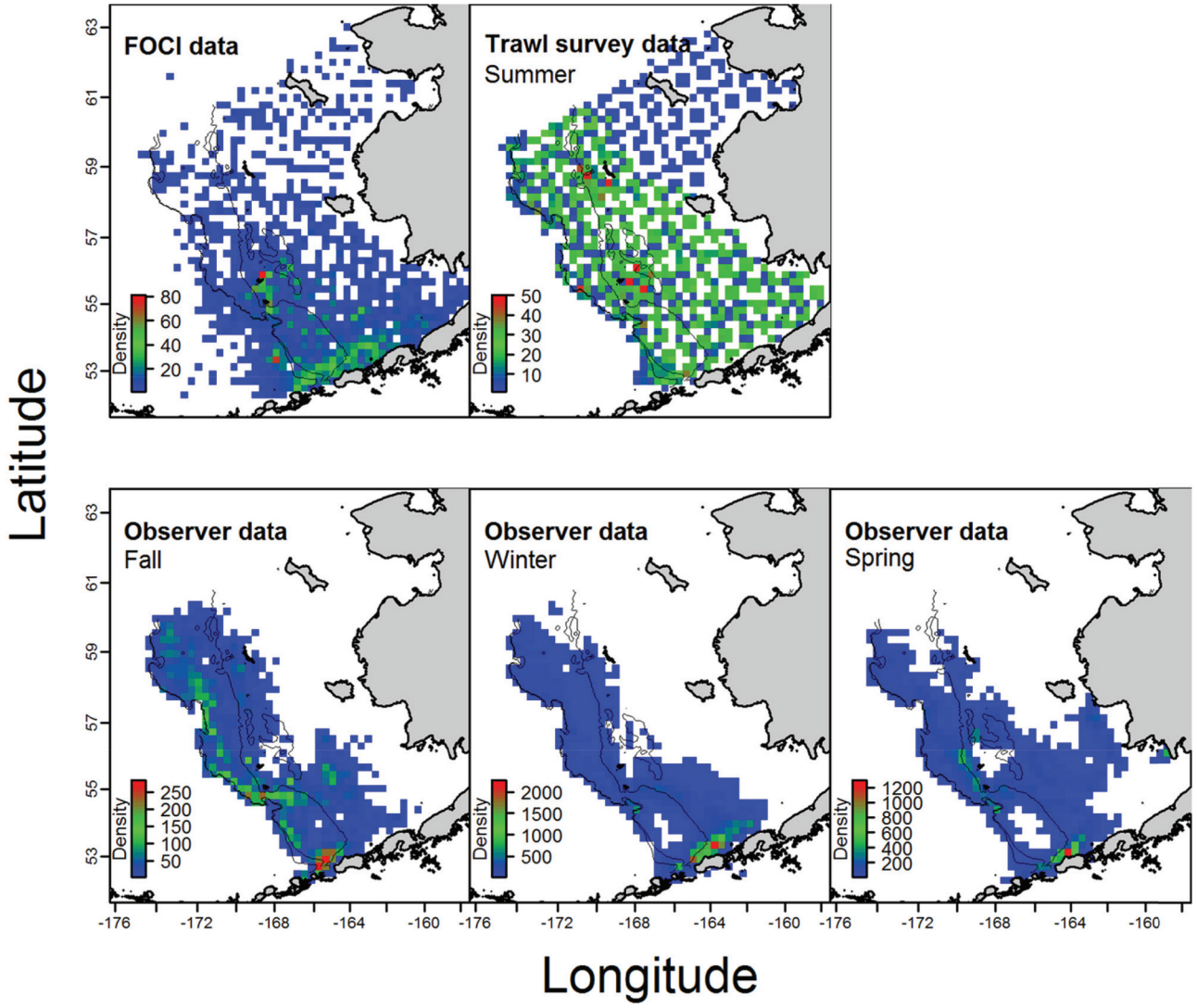

covariates collected on the bottom trawl survey plus some derived and modeled variables (Table 1). Observed, derived, or modeled point values were interpolated to regular spatial grids (rasters) on scales ranging from 100 m × 100 m to 1 km × 1 km using inverse distance weighting (Watson and Philip 1985) or ordinary kriging (Venables and Ripley 2002) with an exponential semivariogram model (Fig. 3). The potential of independent habitat covariates to influence the distribution of life stages of the fishes and invertebrates in the region was considered when identifying which predictors to include in the initial model formulations. For example, ELHS of *Atheresthes* spp. (i.e., eggs and larvae) are pelagic and complete their development in the water column. Therefore, surface water temperature, surface current speed, and surface current direction were among the covariates chosen to formulate the ELHS models. Additionally, surface current direction variability was considered as an indication of potential eddy vorticity and was incorporated into these models. The covariates describing surface currents and temperature were derived from the regional ocean modeling system (ROMS) run for the period 1969–2005 (Danielson et al. 2011). Monthly data originated from a 10 km × 10 km grid. The ROMS modeled data used were temporally synched to the months when the ELHS were present in the water column. For example, *Atheresthes* spp. larvae were collected on ichthyoplankton surveys in the eastern Bering Sea from February until September, so the ROMS data from these months were input to the SDM.

Prior to formulating and then selecting the best-fitting SDMs, we evaluated candidate covariates to address levels of collinearity. The relatively high Pearson correlation between latitude and longitude (r = 0.60) resulted in our including geographic location in the SDMs as a bivariate interaction term (longitude × latitude). Spatial modeling exercises such as presented here commonly use a location variable to represent geographic position and to incorporate potential spatial autocorrelation in the residuals (Swartzman et al. 1992; Denis et al. 2002; Politou et al. 2008). However, use of a location variable precludes extension of the models outside the area of interest for this study (i.e., the eastern Bering Sea LME and northern Bering Sea). Water column irradiance and rugosity were correlated with depth, so these two variables were removed from the suite of habitat covariates used to formulate the SDMs. Variance inflation factors were calculated and assessed using the method described by Zuur et al. (2009) and were determined to be acceptable

Table 1. Variables used in modeling the distributions of fishes and invertebrates in the eastern Bering Sea.

		Definitions			
Variable	Unit	Parameterization	Prediction	Interpolation method	Source
Position	Eastings, northings	Latitude and longitude of bottom trawl hauls in Alaska Albers Equal Area Conic projection corrected for the position of the trawl net relative to the vessel	Latitude and longitude raster surfaces	—	LORAN, GPS, and DGPS collected at bottom trawl haul stations
Depth	m	Bottom depth measured at the trawl station	Bathymetry of the seafloor based on digitized and position-corrected National Ocean Service charts	Linear interpolation	Bottom trawl haul depth measurements: M. Zimmermann, unpublished data
Slope	Percent	Raster of maximum difference between a depth measurement and its adjacent neighbors	Raster of the maximum difference between a depth measurement and its adjacent neighbors	—	M. Zimmermann, unpublished data
Bottom temperature	°C	Bottom temperature measured at the sampling station concurrent with the trawling event	Summer bottom temperatures measured during bottom trawl surveys from 1996 to 2010 and kriged over the survey area	Ordinary kriging	Temperature data collected at bottom trawl hauls
Surface temperature	°C	Ocean surface temperature predicted from the ROMS model during the years 1970–2004 and averaged on a 10 km × 10 km grid	Ocean surface temperature predicted from the ROMS model during the years 1970–2004 and averaged on a 10 km × 10 km grid	Inverse distance weighting	Danielson et al. 2011[a]
Ocean color	Carbon·m^{-2}·day^{-1}	Net primary production in surface waters in May to September averaged by 1080 × 2160 grid cells then averaged across years (2002–2011)	Net primary production in surface waters in May to September averaged by 1080 × 2160 grid cells then averaged across years (2002–2011)	Inverse distance weighting	Behrenfeld and Falkowski 1997
Mean bottom ocean current	m·s^{-1}	Seafloor ocean current speed predicted from the ROMS model during the years 1970–2004 and averaged on a 10 km × 10 km grid	Seafloor ocean current speed predicted from the ROMS model during the years 1970–2004 and averaged on a 10 km × 10 km grid	Inverse distance weighting	Danielson et al. 2011
Maximum tidal current	cm·s^{-1}	Maximum of the predicted tidal current at each bottom trawl location over a 1-year cycle	Maximum of the predicted tidal current at each bottom trawl location over a 1-year cycle	Ordinary kriging	Egbert and Erofeeva 2002
Mean surface ocean current speed	m·s^{-1}	Surface ocean current speed predicted from the ROMS model during the years 1970–2004 and averaged on a 10 km × 10 km grid	Surface ocean current speed predicted from the ROMS model during the years 1970–2004 and averaged on a 10 km × 10 km grid	Inverse distance weighting	Danielson et al. 2011[a]
Mean surface ocean current direction	Angle	Surface ocean current direction predicted from the ROMS model during the years 1970–2004 and averaged on a 10 km × 10 km grid	Surface ocean current direction predicted from the ROMS model during the years 1970–2004 and averaged on a 10 km × 10 km grid	Inverse distance weighting	Danielson et al. 2011[a]
Surface ocean current direction variability	—	Variability in surface ocean current direction predicted from the ROMS model during the years 1970–2004 and averaged on a 10 km × 10 km grid	Variability in surface ocean current direction predicted from the ROMS model during the years 1970–2004 and averaged on a 10 km × 10 km grid	Inverse distance weighting	Danielson et al. 2011[a]

Table 1 (*concluded*).

Variable	Unit	Definitions		Interpolation method	Source
		Parameterization	Prediction		
Sediment grain size (phi)	—	Sediment grain size derived from historical bottom sampling in the eastern Bering Sea compiled in the EBSSED database	Sediment grain size derived from historical bottom sampling in the eastern Bering Sea compiled in the EBSSED database	Ordinary kriging	Smith and McConnaughey 1999
Coral presence or absence	—	Coral presence or absence in bottom trawl catch	Raster of predicted presence or absence of coral	—	Bottom trawl haul catch and Rooper et al. 2016[b]
Sponge presence or absence	—	Sponge presence or absence in bottom trawl catch	Raster of predicted presence or absence of sponge	—	Bottom trawl haul catch and Rooper et al. 2016[b]
Pennatulacean presence or absence	—	Pennatulacean presence or absence in bottom trawl catch	Raster of predicted presence or absence of pennatulacean	—	Bottom trawl haul catch and Rooper et al. 2016[b]

[a]Used to model egg, larval, and early juvenile stages only.
[b]Used to model bottom trawl survey data only.

(<5.0) ranging from 1.05 to 3.41 for the remaining covariates (Table 2). Prior to modeling runs, we randomly selected training (80% of observations) and testing (20% of observations) data sets for each of the data types. For the bottom trawl hauls (where presence, absence, and abundance were reliably measured in each catch), the training and testing data sets were the same across species. For the presence-only data (i.e., ELHS and observer data), a new division of training and testing data was chosen for each species' season and life stage modeled. For all dependent data types, the training data were used to parameterize and select the best-fitting model, and the remaining 20% held back were used to test and validate the model fit.

Geographic position was collected during each bottom trawl haul. Start and end positions for the vessel during the on-bottom portion of the trawl haul were collected using a GPS receiver on the vessel. Vessel position was corrected to the position of the bottom trawl by triangulating how far the net was behind the vessel (based on the seafloor depth and the wire out) and subtracting this distance from the vessel position in the direction of travel of the bottom trawl haul. We assumed that the bottom trawl was directly behind the vessel during the tow and that all bottom trawl hauls were conducted in a straight line from the beginning point to the end point. The midpoint of the trawl path between the start and end positions was used as the location variable in the models. The longitude and latitude data for each tow (and all other geographical data, including the raster layers described here) were projected into Alaska Albers Equal Area Conic projection (standard parallels = 55°N and 65°N and center longitude = 154°W), and degrees of latitude and longitude were transformed into eastings and northings for modeling. The location variable was used to capture any significant spatial trends in the bottom trawl survey catches across the eastern Bering Sea.

A bathymetry raster for the eastern Bering Sea was produced for these analyses using soundings from National Ocean Service smooth sheets and a variety of other sources (M. Zimmermann, National Marine Fisheries Service Alaska Fisheries Science Center, unpublished data, 2014). Soundings on National Ocean Service smooth sheets were digitized and compiled according to the methods in Zimmermann and Benson (2013). These point data were linearly interpolated to create a triangular irregular network, which was converted into a 100 m × 100 m grid (raster surface) using local area weighting called natural neighbors in ArcMAP (ArcMap Desktop; Environmental Systems Research Institute (2009), Redlands, California). Empty spaces in the grid were filled using data compiled by AKRO (S. Lewis, Alaska Regional Office, personal communication, 2014). Slope was derived from the 100 m × 100 m bathymetry raster. Slope for each raster grid cell was computed as the maximum difference between the depth at a cell and its surrounding cells using the raster package (Hijmans et al. 2015) in R (R Core Team 2013). For the analysis of ELHS data, the bathymetry and slope layers were averaged over a 1 km × 1 km grid.

Mean ocean productivity in grams of carbon per square metre per day (carbon·m^{-2}·day^{-1}) was used to indicate primary productivity at each of the bottom trawl survey sites. We used moderate resolution imaging spectroradiometer (MODIS) satellite ocean color from the eastern Bering Sea over five spring–summer months (May–September) covering 8 years (2003–2011) of data collection (Behrenfeld and Falkowski 1997). These data were downloaded from Oregon State University's Ocean Productivity website (URL: http://www.science.oregonstate.edu/ocean.productivity/, accessed 15 November 2016), were averaged by cell and by month, and then averaged again by cell and by year (to account for differences in the number of samples within each cell). The means were interpolated to 100 m × 100 m raster grids using inverse distance weighting (Fig. 3). The mean value in the grid cell beneath each bottom trawl survey tow was extracted from the raster and used for prediction.

Fig. 3. Distribution of habitat covariates used to model essential fish habitat for groundfishes and invertebrates in the eastern and northern Bering Sea. See Table 1 for detailed descriptions, data sources, and units for each habitat variable.

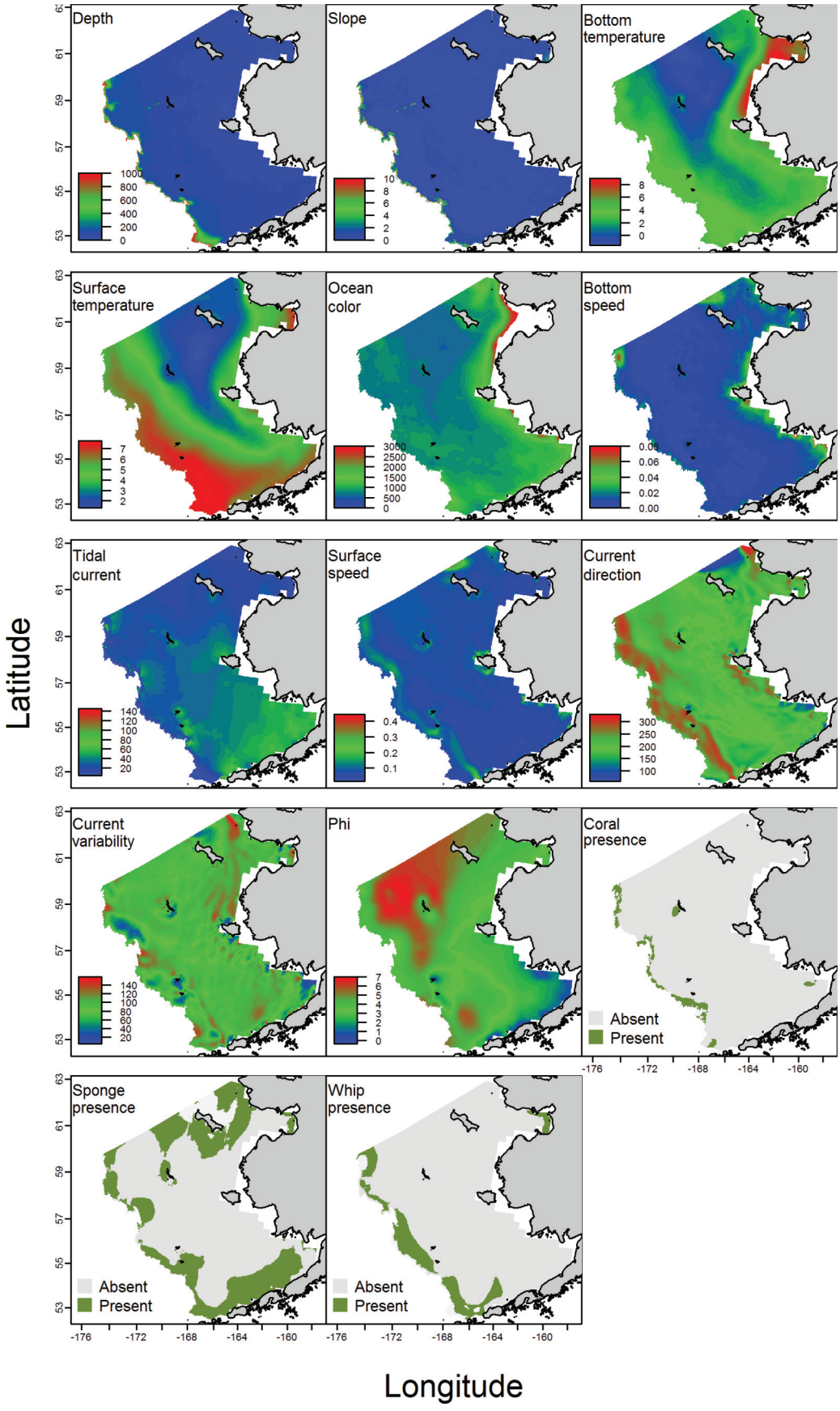

Table 2. Variance inflation factors among habitat covariates from the eastern and northern Bering Sea NMFS Alaska Fisheries Science Center summer bottom trawl surveys.

	Variance inflation factors		
Variable	RACE-GAP	VOE-CIA	EcoFOCI
Depth	2.79	2.73	3.23
Slope	2.10	2.12	1.63
Bottom temperature	1.65	1.73	
Ocean color	2.01	1.73	1.11
Mean bottom ocean current speed	1.68	1.23	
Maximum tidal current speed	3.41	2.35	2.08
Sediment grain size (phi)	3.24	2.62	
Coral presence–absence	1.10		
Sponge presence–absence	1.17		
Pennatulacean presence–absence	1.05		
Surface temperature			1.30
Mean surface ocean current speed			1.38
Surface ocean current direction variability			1.41

Note: RACE-GAP, Resource Assessment and Conservation Engineering – Groundfish Assessment Program; VOE-CIA, VMS–Observer Enabled Catch-in-Areas commercial catch observations; EcoFOCI, Ecosystems and Fisheries-Oceanography Cooperative Investigations ichthyoplankton surveys.

Sediment grain size from the National Geophysical Data Center Seafloor Sediment Grain Size database (Smith and McConnaughey 1999; URL: http://ngdc.noaa.gov/geosamples/, accessed 15 November 2016) was also used as a covariate to predict bottom trawl survey catches. Mean grain size (mm) is expressed as phi, which is the negative $\log_2$-transform of grain size (i.e., a large phi indicates fine grains). The sampling tools for this sediment information were bottom grabs and corers, which do not distinguish boulder or bedrock habitat, and as a result, we did not consider these habitat types. The grain size and sorting values from the sediment data (n = 803) were kriged (Fig. 3) using an exponential model (Venables and Ripley 2002) representing the best fit to the semivariogram of both grain size and sorting values.

Bottom depth and temperature were routinely collected at each trawl haul site on the eastern Bering Sea bottom trawl survey between 1982 and 2014, but different instruments were used to measure these values through the years (Buckley et al. 2009). From 1982 to 1992, depth and temperature were recorded using expendable bathythermographs. In 1993, the expendable bathythermographs were replaced by the Brancker XL200 digital bathythermographic data logger (Richard Brancker Research, Ltd., Kanata, Ontario, Canada), which was mounted on the headrope of the trawl net. With the advent of continuous temperature and depth recording at the trawl net, the survey began reporting on-bottom depth and temperature averaged over the trawl haul duration. Starting in 2004, the Brancker data logger was replaced by the SeaBird SBE-39 microbathythermograph (Sea-Bird Electronics, Inc., Bellevue, Washington). In 1993–1995, mean gear depth measured at the headrope was equated with bottom depth. Since 1996, mean gear depth has been added to mean net height during the on-bottom period of the trawl to estimate mean bottom depth; mean net heights for the RACE-GAP trawl net ranged from 2 m to approximately 4 m during the survey years included in our analyses.

One focus of this work was to produce single, species-specific distribution maps that represented average conditions over time to refine extant EFH descriptions for spatial planning and fishery management. Once a best-fitting SDM was identified, rasters of retained covariates, averaged over the survey years considered, were used as model inputs to predict species distribution. For example, we parameterized our SDMs with point observations of temperature, but predicted species distribution from the SDM using a multiyear temperature mean. The estimated slope derived from the bathymetry raster at each bottom trawl haul site was used as a habitat covariate as well, but the slope raster derived from bathymetry was used for prediction. Mean bottom temperatures from each trawl haul across survey years were interpolated to a 100 m × 100 m grid of the eastern Bering Sea (Fig. 3) using ordinary kriging with an exponential semivariogram model. The result was a single temperature raster layer used for prediction that reflects the mean temperature conditions at the bottom trawls over the survey years.

Two measures of water movement and its potential interaction with the seafloor were used as habitat covariates in modeling and prediction. One covariate was the maximum tidal speed at the site of each bottom trawl haul. Tidal speeds were estimated for a lunar year (369 consecutive days between 1 January 2009 and 4 January 2010) using a tidal inversion program parameterized for the eastern Bering Sea on a 1 km × 1 km grid (Egbert and Erofeeva 2002). This tidal prediction model was used to produce a series of tidal currents for spring and neap cycles at each bottom trawl survey location for the lunar year. The maximum of the lunar annual series of predicted tidal current was then extracted at the position of each bottom trawl survey haul. For prediction, maximum tidal current at each bottom trawl survey site was kriged over the eastern Bering Sea using an exponential semivariogram to interpolate a raster of values on a 1 km × 1 km grid (Fig. 3).

The second water movement covariate was the bottom water layer current speed predicted from ROMS model runs 1969–2005 (in Danielson et al. 2011). Long-term current speed and direction were available as points on a 10 km × 10 km grid. The ROMS model was based on a three-dimensional grid with 60 depth tiers for each grid cell. For example, a point at 60 m water depth would have 60 depth bins at 1 m intervals, while a point at 120 m depth would have 60 depth bins at 2 m depth intervals. The current speed and direction for the deepest depth bin at the point closest to the seafloor was used in the SDM. The regularly spaced ROMS data were then interpolated by inverse distance weighting to a 100 m × 100 m cell size raster covering the eastern Bering Sea (Fig. 3) and were used for prediction with the best-fitting SDM. Values from this raster at each bottom trawl station were extracted and the mean value computed for the path of each bottom trawl survey tow.

Previous studies have indicated that biogenic structures formed by benthic invertebrates such as sponges and corals can be important habitat (Heifetz et al. 2005; Malecha et al. 2005; Stone et al. 2011) for temperate marine fishes (Brodeur 2001; Marliave and Challenger 2009; Rooper et al. 2010; Laman et al. 2015). Presence and absence of benthic invertebrates also indicates substratum type (Du Preez and Tunnicliffe 2011), since these animals have to attach to rocks or other hard substrata to survive. Therefore, we included the presence and absence in trawl catches of structure-forming invertebrates (corals, sponges, and pennatulaceans) as binomial factors in the suite of habitat covariates used to formulate the SDMs (Table 1). Rasters used to predict EFH from presence–absence of these benthic invertebrates (Fig. 3) were derived from distribution models for each group (Rooper et al. 2014, 2016, 2017).

We also modeled species distribution using commercial catch observer data (VOE-CIA). The suite of habitat covariates used to parameterize the models used with these data was the same as that for the SDMs that used the RACE-GAP summer bottom surveys, with the exception that we did not include the binomial structure-forming invertebrate factors described above (Table 1). Rasters of covariates used to predict EFH from the observer data were the same as those used with the RACE-GAP bottom trawl survey SDMs.

Modeling methods — ichthyoplankton surveys and commercial observer data

Maximum entropy modeling (MaxEnt: Phillips et al. 2006; Elith et al. 2011) was used to calculate the probability of suitable habitat for species' ELHS and presence in commercial fisheries using distribution data extracted from the EcoFOCI ECODAAT database as

well as the VOE-CIA observer database. The models were implemented in R (R Core Team 2013) using the dismo package (Hijams et al. 2014). MaxEnt models use only presence observations and are based on raster grids of explanatory variables (habitat covariates) and point observations of presence. They predict the probability of suitable habitat based on the co-occurring habitat covariates and species prevalence (e.g., given the depth, temperature, slope, and current speed at each grid cell — what is the probability that this is a suitable location for a Kamchatka flounder?). MaxEnt models were used only when the number of presence observations exceeded 50. While the *N* of 50 is somewhat arbitrary, it does ensure in the 80/20 training/testing system of data we set up that there were at least 10 records in the test data sets for these low prevalence species.

Modeling methods — bottom trawl survey data

Three SDM techniques were applied to the RACE-GAP summer bottom trawl survey data. The technique employed was determined by the prevalence of each species in the overall survey. When the species occurred in >30% of bottom trawl hauls, a generalized additive model (GAM; Hastie and Tibshirani 1986, 1990) was used to describe the relationships between habitat covariates and fourth-root-transformed CPUE. These analyses were conducted in R (R Core Team 2013) using the mgcv package (Wood 2014). For each of the habitat covariates, the degrees of freedom used in the smoothing function were constrained to ≤4 for univariate terms and ≤10 for the bivariate term (geographic location) following the method in Weinberg and Kotwicki (2008) to reduce the chance of overfitting the GAMs. Insignificant terms (based on *p* values) were iteratively removed using backward stepwise term elimination until the generalized cross validation score (GCV) was minimized (Wood 2006). For a species – life-stage combination, the reduced model with the lowest GCV was deemed the best-fitting and was used for validation and prediction.

Hurdle GAMs (hGAMs; Cragg 1971; Barry and Welsh 2002; Potts and Elith 2006), which model presence–absence and abundance separately, are advantageous because they account for overdispersion and zero-inflation commonly seen in field-collected data. In this study, when a species' prevalence in bottom trawl hauls was between 10% and 30% of the catches (70%–90% absent over the study area), the relationships among habitat covariates, presence–absence data, and fourth-root-transformed CPUE were modeled using an hGAM, which was applied in three stages: (1) the probability of presence was predicted from presence–absence data using a GAM and binomial distribution; (2) an optimal threshold probability for presence was determined by balancing the false positive and false negative predictions of species' presence–absence using the PresenceAbsence package in R (Freeman 2010); and (3) a second GAM was constructed for the positive catches to model the relationship between CPUE and the habitat covariates (Manel et al. 2001; Barry and Welsh 2002; Wilson et al. 2005). We used iterative backward stepwise term elimination and minimized the information criterion (the unbiased risk estimator for presence–absence data and the GCV for abundance data) to identify the best-fitting models at stages 1 and 3 above (Chambers and Hastie 1992). Model formulation at each stage started with the same initial suite of habitat covariates; the covariates retained in one model type were typically a subset of those retained in the other. The information developed at each stage of the hGAM was used to make predictions of abundance at locations where presence was predicted (i.e., the probability of presence was equal to or exceeded the threshold established in step 2), and so these are referred to as conditional abundance models. As with the standard GAMs, the number of inflection points for the smoother were limited during model fitting by fixing the maximum degrees of freedom for each habitat covariate.

For settled juveniles and adults from the bottom trawl survey, where the frequency of occurrence in bottom trawl hauls was <10% but more than 50 observations of presence occurred, a MaxEnt model was used to predict the probability of suitable habitat. MaxEnt models of presence-only data for the bottom trawl survey were applied in the same fashion as for the ELHS and the commercial fisheries observer data.

Model validation

We tested the predictive power of the final models in several ways. To test the performance of the best-fitting models, the correlation between predictions and observations was computed. For presence and presence–absence models, the area under the receiver operating characteristic curve (AUC) was computed in R using the auc function in the PresenceAbsence package, which approximates the area under the curve with a Mann–Whitney *U* statistic (Delong et al. 1988). The AUC approximates the probability that a randomly chosen presence observation would have a higher probability of presence than a randomly chosen absence observation. We used the scale of Hosmer and Lemeshow (2005), where an AUC value > 0.5 is estimated to be better than chance, a value > 0.7 is considered acceptable, and values > 0.8 and 0.9 are excellent and outstanding, respectively. Confidence intervals (95%) for the AUC were calculated according to the methodology of DeLong et al. (1988). For abundance SDMs, model performance was directly tested by correlating the predictions with the observations. Model testing was also performed on the random 20% of the data (testing data) withheld a priori, using the same metrics. Because of space limitations, figures showing the model validation results are not included here. However, deviations from model assumptions or models with very poor predictive ability relative to the testing data are highlighted. Where these conditions occur, the predicted distributions may not be robust.

Species distribution maps

Maps of species distribution predicted from habitat-based models were used to refine existing descriptions of EFH. These maps were produced as population quantiles from predictions of the distribution of suitable habitat (in cases where MaxEnt was used) or predictions of the distribution of abundance (for species where CPUE was modeled using either a GAM or hGAM). For each map of model predictions, 300 000 points were randomly sampled from the raster surface. These values were then ordered by cumulative distribution; zero abundance values and probabilities of suitable habitat <0.05 were removed. Four population quantiles were selected from these cumulative distributions (5%, 25%, 50%, and 75%). These quantiles were then used as break points to translate the model predictions (maps of suitable habitat or abundance) into maps of the distribution quantiles. For example, if the 5% quantile of species A was 0.024 individuals·ha^{-1}, then this meant that 95% of the population occurred at values higher than 0.024. Similarly, a 75% quantile of species A at 2.1 individuals·ha^{-1} meant that values above 2.1 represented the top 25% of the population of predictions, or the highest predicted areas of abundance. The four population quantiles for each species, life history stage, and season were mapped to show the distribution of the areas containing 95%, 75%, 50%, and 25% of the population. It is important to note that these values were chosen somewhat arbitrarily, with the exception of the 95% level, which is the current definition of EFH in Alaska (URL: http://www.npfmc.org/habitat-protections/essential-fish-habitat-efh/, accessed 15 November 2016); other values could be equally appropriate.

The case study presented here was part of a larger project that used SDM techniques to refine descriptions of EFH for all federally managed species in the eastern Bering Sea (Table 3). In addition to the results from our case study of *Atheresthes* spp. ELHS and Kamchatka flounder settled juveniles and adults, we present EFH maps for selected adult flatfishes, roundfishes, and crabs in the eastern Bering Sea. In total, our larger eastern Bering Sea study redescribed the EFH of more than two dozen species of fishes and

Table 3. US federally managed species for which distribution models have been successfully constructed for different life history stages.

Species	Eggs	Larvae	Pelagic juveniles	Settled juveniles	Adults
Anoplopoma fimbria, sablefish					
Atheresthes sp.					
Atheresthes evermanni, Kamchatka flounder					
Atheresthes stomias, arrowtooth flounder					
Bathyraja aleutica, Aleutian skate					
Bathyraja interrupta, Bering skate					
Bathyraja parmifera, Alaska skate					
Gadus chalcogrammus, walleye pollock					
Gadus macrocephalus, Pacific cod					
Glyptocephalus zachirus, rex sole					
Hemilepidotus jordani, yellow Irish lord					
Hemitripterus bolini, bigmouth sculpin					
Hippoglossoides elassodon, flathead sole					
Lepidopsetta bilineata, southern rock sole					
Lepidopsetta polyxystra, northern rock sole					
Limanda aspera, yellowfin sole					
Microstomus pacificus, Dover sole					
Myoxocephalus polyacanthocephalus, great sculpin					
Pleurogrammus monopterygius, Atka mackerel					
Pleuronectes quadrituberculatus, Alaska plaice					
Reinhardtius hippoglossoides, Greenland turbot					
Sebastes spp., rockfishes					
Rougheye–blackspotted rockfish complex					
Sebastes aleutianus, rougheye rockfish					
Sebastes alutus, Pacific ocean perch					
Sebastes borealis, shortraker rockfish					
Sebastes melanostictus, blackspotted rockfish					
Sebastes polyspinis, northern rockfish					
Sebastes variabilis, dusky rockfish					
Sebastolobus spp., thornyheads					
Sebastolobus alascanus, shortspine thornyhead					
Chionoecetes bairdi, southern Tanner crab					
Chionoecetes opilio, snow crab					
Octopus (unidentified)					
Paralithodes camtschaticus, red king crab					
Paralithodes platypus, blue king crab					

Note: Blank cells indicate insufficient data available or not applicable; medium shading indicates presence or presence–absence models; darkest shading indicates density (CPUE) models.

crabs, along with other taxonomic groups (i.e., three genera of fish ELHS, the commercial catch rockfish complex "blackspotted–rougheye" (*Sebastes melanostictus* – *Sebastes aleutianus*), and unidentified octopus).

Results

Eggs, larvae, and pelagic juveniles of *Atheresthes* spp. were collected in the ichthyoplankton surveys of the eastern Bering Sea, but the eggs and pelagic juveniles occurred in numbers too low to qualify for distribution modeling (<50 occurrences each). Larvae were sufficiently prevalent on ichthyoplankton surveys from February to September (n = 534 occurrences) to model their distribution (Fig. 4). MaxEnt model predictions of suitable larval *Atheresthes* spp. habitat extended from the Bering Canyon northward to around Pribilof Canyon and eastward onto the middle shelf. The most important habitat covariate determining the distribution of suitable larval *Atheresthes* spp. habitat was sea surface temperature (relative importance = 82.3%). Following the criteria described earlier, the model fits were outstanding to the training (AUC = 0.97) and testing (AUC = 0.92) data. The percentage of cases correctly classified was high in both the training and testing data sets at 90% and 92%, respectively (Table 4).

Settled juvenile Kamchatka flounder were sufficiently prevalent at eastern Bering Sea stations (~40%) to qualify for a standard GAM SDM. The best-fitting model explained 60.6% of the deviance in their CPUE from the RACE-GAP bottom trawl survey (Table 5; Fig. 5). Geographic location, bottom depth, and bottom temperature were the most significant covariates predicting settled juvenile abundance. Their abundance increased from east to west across the outer shelf with increasing depth and bottom temperature. Juvenile Kamchatka flounder abundance also decreased with increasing local slope and increased in the presence of sponges, corals, and pennatulaceans. The R^2 of the fits to the training and test data were 0.61 and 0.60, respectively. The areas of highest predicted settled juvenile Kamchatka flounder abundance were along the outer continental shelf and upper continental slope.

The prevalence of adult Kamchatka flounder at RACE-GAP summer bottom trawl survey stations in the eastern and northern Bering Sea was between 10% and 30%, so an hGAM was used to characterize their distribution (Table 6). The highest probability of adult Kamchatka flounder presence was predicted to occur over 200–1000 m depths along the upper continental slope (Fig. 6). The seven habitat covariates retained in the best-fitting presence–absence GAM explained 46.6% of the deviance in adult Kamchatka flounder distribution in RACE-GAP surveys. The most significant predictors retained in the model were bottom depth, bottom temperature, and geographic location. The probability of encountering adult Kamchatka flounder increased from east to west across the outer continental shelf and upper continental slope as bottom

Fig. 4. Larval *Atheresthes* spp. presence in ichthyoplankton surveys of the eastern Bering Sea (left panel) from February to September, response curves for maximum entropy models predicting suitable habitat for *Atheresthes* spp. larvae (bottom panels), and predicted distribution of probability of suitable larval *Atheresthes* spp. habitat across the eastern and northern Bering Sea (right panel).

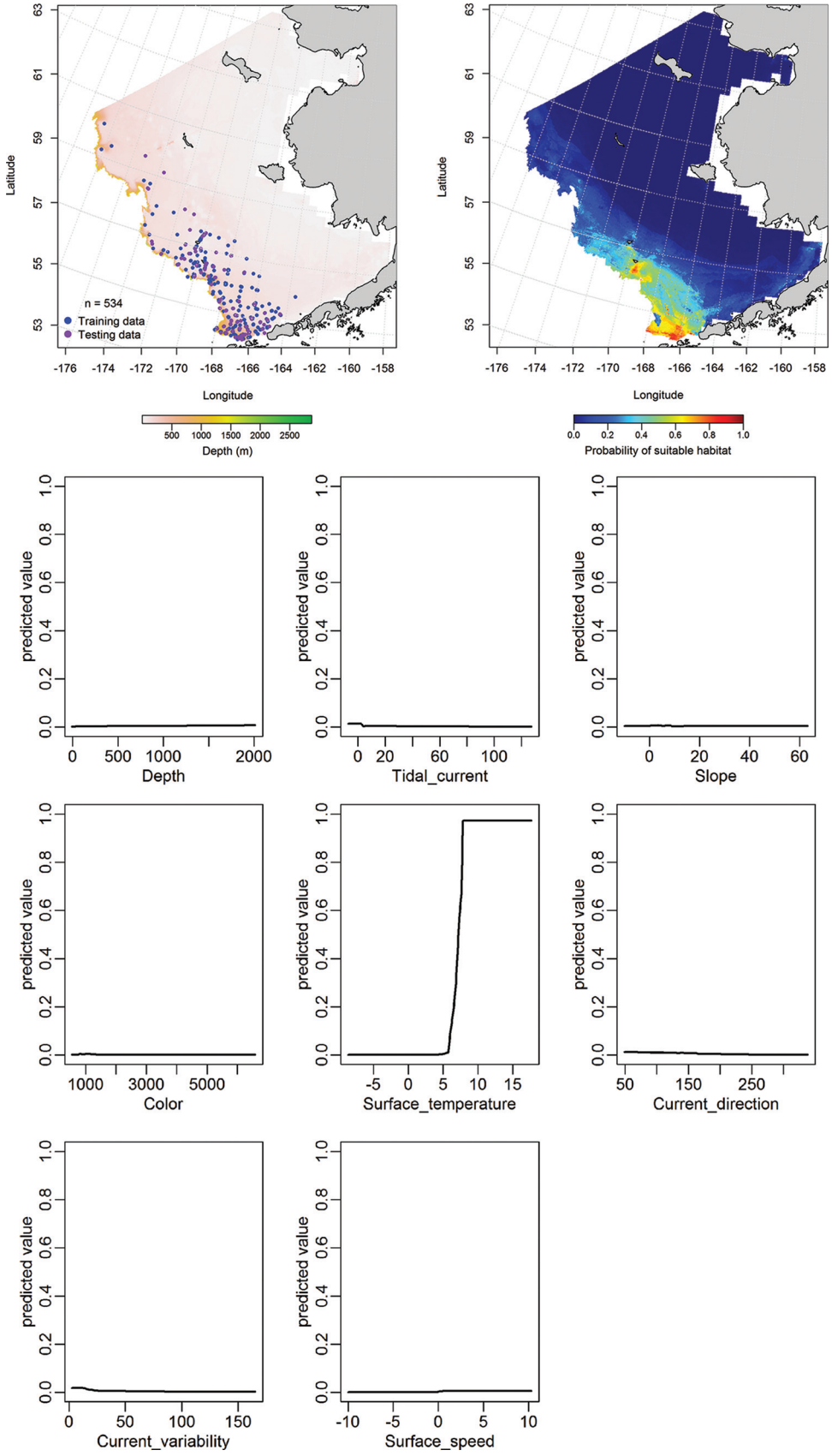

Table 4. Maximum entropy species distribution modeling (MaxEnt) results for larval *Atheresthes* spp. stages and commercial catches of Kamchatka flounder (*Atheresthes evermanni*) during fall, winter, and spring in the eastern and northern Bering Sea, indicating relative importance of independent habitat predictor variables and results of model validation.

Habitat covariate	Relative importance
Larval stages	
Surface temperature	82.3
Depth	8.0
Ocean color	2.4
Slope	2.1
Current direction	2.1
Current speed	1.4
Current variability	1.3
Training data	
AUC	0.97
PCC	0.90
Test data	
AUC	0.92
PCC	0.92
Commercial catches — fall	
Bottom depth	69.9
Bottom temperature	20.3
Ocean color	6.9
phi	0.8
Current speed	0.2
Slope	0.1
Training data	
AUC	0.88
PCC	0.80
Test data	
AUC	0.80
PCC	0.80
Commercial catches — winter	
Bottom depth	60.5
Bottom temperature	32.6
Ocean color	2.3
phi	0.6
Current speed	0.3
Slope	0.1
Training data	
AUC	0.93
PCC	0.86
Test data	
AUC	0.85
PCC	0.85
Commercial catches — spring	
Bottom depth	52.9
Bottom temperature	32.5
Ocean color	1.7
Current speed	0.8
phi	0.7
Slope	0.1
Training data	
AUC	0.93
PCC	0.86
Test data	
AUC	0.85
PCC	0.85

Note: AUC, area under receiver operating characteristic curve; PCC, percent correctly classified.

Table 5. Generalized additive modeling (GAM) results for settled juvenile Kamchatka flounder (*Atheresthes evermanni*) captured during RACE-GAP summer bottom trawl surveys of the eastern and northern Bering Sea.

Habitat covariate	EDF	*p* value
Longitude–latitude	9.0	<0.001
Bottom depth	3.0	<0.001
Bottom temperature	2.6	<0.001
Slope	3.0	<0.001
Maximum tidal current	2.6	<0.001
Pennatulaceans present	1	<0.001
Sediment grain size	2.7	<0.001
Sponge present	1	<0.001
Ocean color	2.0	<0.001
Current speed	2.3	0.003
Coral present	1	0.021
Training data R^2	0.61	
Test data R^2	0.60	

Note: Data include estimated degrees of freedom (EDF) and probability (*p*) values for each habitat covariate retained in the best-fitting model (longitude–latitude is a bivariate interaction term) with overall correlation coefficient (R^2) for training and testing data sets.

temperature and bottom depth increased. This GAM was an outstanding fit to the training data (AUC = 0.92) and correctly classified 84% of presence–absence cases. Using the test data, the best-fitting GAM was validated with an outstanding fit (AUC = 0.93), correctly classifying 85% of cases. The optimal probability threshold for adult Kamchatka presence was 0.23. The best-fitting conditional abundance GAM explained 42.8% of the deviance in adult Kamchatka flounder CPUE. Abundance where present increased from west to east along the upper continental slope, with the highest abundances predicted around the head of Pribilof Canyon. The most significant of the nine habitat covariates retained in the model were bottom depth, geographic location, and coral presence. The model fits to the training and test data were about equal (R^2 = 0.43 and 0.42, respectively). The seven covariates retained in the presence–absence GAM were a subset of the nine covariates retained in the conditional abundance GAM with two of the three most influential predictors of distribution (bottom depth and geographic location) retained in the conditional abundance GAM.

For Kamchatka flounder in commercial catches from the eastern Bering Sea during the fall, bottom depth and bottom temperature were the most important covariates (combined relative importance = 83.5%) in the MaxEnt model (Table 4). This model was an excellent fit to the training data (AUC = 0.88) and correctly predicted 80% of cases, with most of the Kamchatka flounder habitat along the outer shelf and around the heads of the major submarine canyons (Fig. 7). Model validation with the test data did not fit as well, but was still excellent (AUC = 0.80) with 80% of cases correctly classified. In winter, depth and bottom temperature were the most important of the habitat covariates with a combined relative importance of 93.1%. Similar to fall, the highest probability of suitable habitat for Kamchatka flounder was predicted along the outer shelf and upper slope. The model was an outstanding fit to the training data (AUC = 0.93), with 86% of cases correctly predicted. Model validation with the test data did not fit as well, but was still excellent (AUC = 0.85) with 85% of cases correctly classified. In the spring, depth and bottom temperature comprised 85.4% of the relative importance of the covariates in the MaxEnt model. Similar to winter and fall, the highest probabilities of suitable habitat were predicted to be on the outer shelf and upper slope. The model fit to the training data was outstanding (AUC = 0.93), with 86% of cases correctly predicted. Model

Fig. 5. Distribution of settled juvenile Kamchatka flounder (*Atheresthes evermanni*) in RACE-GAP summer bottom trawl surveys (left panel) alongside effects of retained habitat covariates on the best-fitting generalized additive model (GAM; bottom panels) and their predicted abundance across the eastern and northern Bering Sea (right panel).

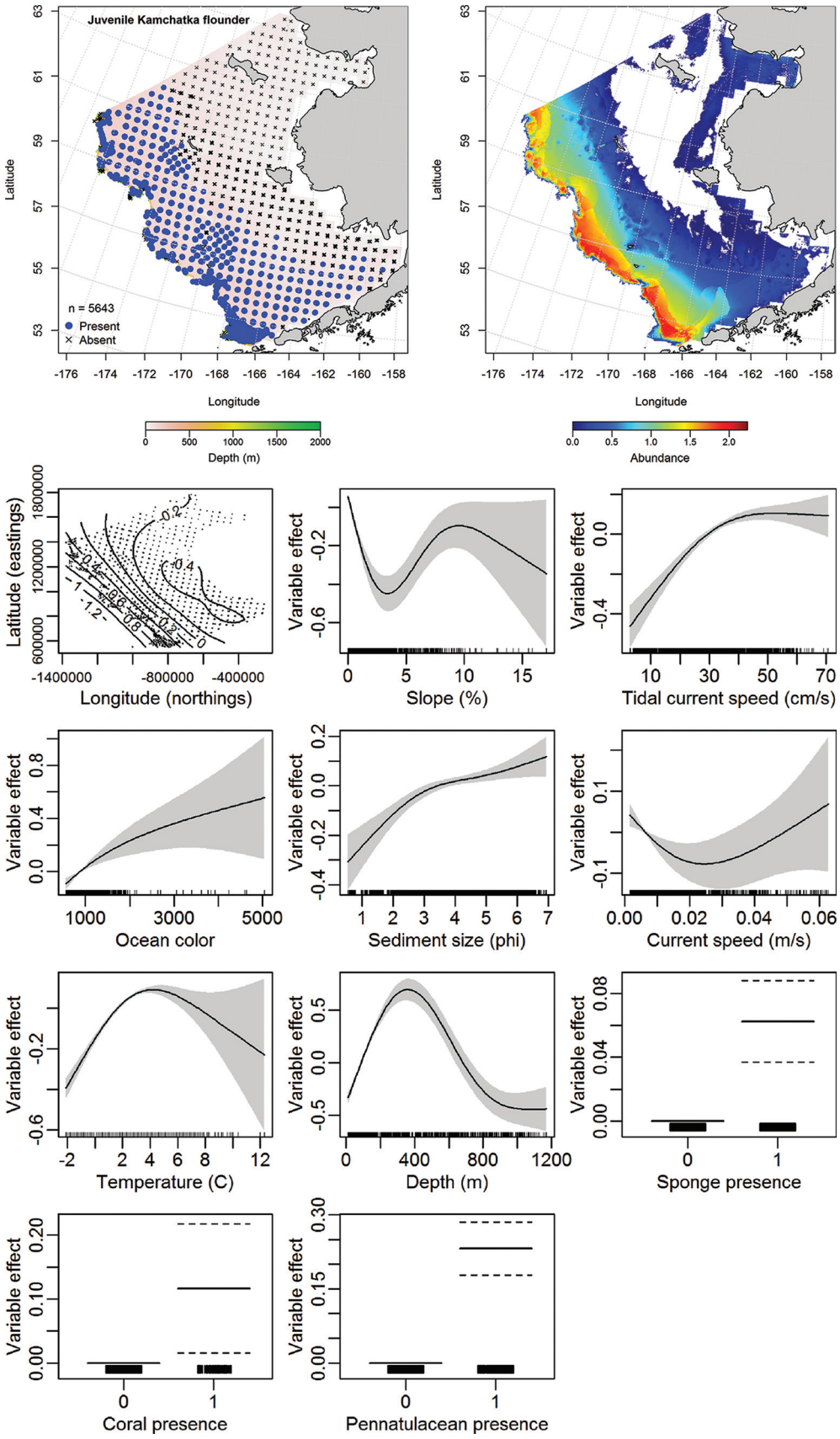

Table 6. Hurdle generalized additive modeling (hGAM) results for adult Kamchatka flounder (*Atheresthes evermanni*) captured during RACE-GAP summer bottom trawl surveys of the eastern and northern Bering Sea.

Habitat covariate	EDF	*p* value
Presence–absence		
Bottom depth	3.0	<0.001
Bottom temperature	3.0	<0.001
Longitude–latitude	9.0	<0.001
Sediment grain size	2.2	<0.001
Maximum tidal current	2.4	0.001
Slope	2.9	0.010
Current speed	2.7	0.198
Optimum threshold	0.23	
Training data		
AUC	0.92	
PCC	0.84	
Test data		
AUC	0.93	
PCC	0.85	
CPUE		
Bottom depth	3.0	<0.001
Longitude–latitude	8.5	<0.001
Coral present	1.0	<0.001
Temperature	2.8	0.001
Sediment grain size	1.0	0.022
Ocean color	1.6	0.036
Current speed	2.0	0.116
Slope	2.6	0.148
Maximum tidal current	2.7	0.148
Training data R^2	0.43	
Test data R^2	0.42	

Note: Data include estimated degrees of freedom (EDF) and probability (*p*) values for retained habitat covariates (longitude–latitude is a bivariate interaction term) along with the optimum presence probability threshold (Optimum threshold) for the presence–absence GAM, the area under the receiver operating characteristic curve (AUC), and the percentage of cases correctly classified (PCC) from training and test data sets. Additionally, the correlation coefficient (R^2) from the best-fitting abundance (CPUE) GAM are indicated for the training and test data sets.

validation with the test data did not fit as well, but was still excellent (AUC = 0.85) with 85% of cases correctly classified.

A single EFH map for each life stage and season was generated from the SDM results (Fig. 8). Overall, essential habitat predicted with SDMs for the ELHS and later life stages of Kamchatka flounder extends the length of the continental shelf of the eastern Bering Sea from the Alaska Peninsula to the US–Russia Convention Line and is somewhat more dispersed for the earlier life stages (i.e., larvae and settled juveniles). Core larval *Atheresthes* spp. habitat (the top 25% of predictions) was distributed primarily across the central and southern portions of the outer and middle shelf and the upper continental slope. Settled juvenile Kamchatka flounder core habitat covered a larger area than that of larval *Atheresthes* spp. and extended the length of the survey area from southeast to northwest onto the inner shelf in places. Core habitat for adult Kamchatka flounder was generally constrained to the upper continental slope around the heads of submarine canyons and was reflected in the results of the commercial observer data SDM. Essential habitat predicted from the commercial catch showed some seasonal differences that may reflect targeted fishing activities, but overall patterns of distribution predicted from these data were similar across the three seasons analyzed.

From the broader study, SDM-predicted EFH for five selected flatfish species shared some similarities in patterns of distribution (Fig. 9). Adult arrowtooth flounder, northern rock sole (*Lepidopsetta polyxystra*), Alaska plaice (*Pleuronectes quadrituberculatus*), and yellowfin sole summertime distribution overlapped extensively in the eastern Bering Sea, but arrowtooth flounder core habitat was deeper (>100 m) than that of the other three species listed. Fall, winter, and spring EFH were generated from the VOE-CIA data and generally reflect directed fishing activity for that time of the year. The pattern of Greenland turbot (i.e., Greenland halibut, *Reinhardtius hippoglossoides*) distribution was distinctly different than that of the other four selected flatfishes, although there was still some overlap. Core Greenland turbot habitat was deeper and in a relatively narrow band along the continental shelf, which was more similar to habitat of Kamchatka flounder than to that of the other four selected flatfishes.

Roundfish EFH in the eastern Bering Sea was redescribed in the larger study using SDMs. There were basically two patterns of EFH distribution among the five selected roundfish species presented here (Fig. 10). Adult walleye pollock (*Gadus chalcogrammus*) and Pacific cod (*Gadus macrocephalus*) EFH extended from the inner to the outer shelf in summer RACE-GAP surveys, and this pattern was generally confirmed in the fall, winter, and spring commercial fishery observations. The distribution of adult Pacific ocean perch (*Sebastes alutus*), shortspine thornyhead (*Sebastolobus alascanus*), and sablefish (*Anoplopoma fimbria*) EFH was much more constrained and primarily occurred on the outer shelf and along the shelf break with some seasonal extension onto the middle shelf. Core habitat of walleye pollock and Pacific cod was similarly located over the middle and outer shelf between the Alaska Peninsula and the US–Russia Convention Line. Much of the core habitat for the remaining three species overlapped over the outer shelf and shelf break both in summer RACE-GAP surveys and in commercial catches from the other seasons.

The distribution of EFH for crabs in the eastern Bering Sea during summer months demonstrated how the four most common species have fairly distinct distributions at this time of year (Fig. 11). Red king crab (*Paralithodes camtschaticus*) EFH tended to be inshore, while blue king crab (*Paralithodes platypus*) were mostly found in shallow areas around the islands in the middle of the shelf (i.e., the Pribilof Islands and St. Matthews Island). Southern Tanner (*Chionoecetes bairdi*) and opilio (*Chionoecetes opilio*) crab both tended to be dispersed across the shelf, with opilio EFH more prevalent in the north. Blue king crab displayed summer–fall and winter–spring patterns of EFH distribution. The summer–fall pattern for blue king crab seems to be unique to this species among the four crabs presented here and is focused in the vicinity of the Pribilof and St. Matthews Islands. Much of the core habitat for all four of these species overlaps in Bristol Bay to some degree.

Discussion

Spatial predictions of larval *Atheresthes* spp. and juvenile and adult Kamchatka flounder distribution and abundance using SDMs provide an effective framework for describing EFH in Alaska for management purposes. Like those in the case study we have presented here, most of the SDMs we employed consistently explained a large fraction of the variability in the distribution and abundance data, and the models were successfully validated. The habitat covariate with the greatest influence over larval *Atheresthes* spp. distribution was sea surface temperature, and relatively warmer waters over the southeastern outer shelf of the eastern Bering Sea held the highest probability for suitable habitat of this life stage. Similarly, juvenile Kamchatka flounder abundance was predicted to be highest under similar thermal conditions in the same region. The ontogenetic proximity of these two life stages and the geographic closeness of their predicted distributions supports the necessity for spatial connectivity between life stages posited by Walsh et al. (2015) and is suggestive of realism in our model results (i.e., larval and juvenile core habitats are in relatively close proximity and share similar environmental conditions). Additional

Fig. 6. Distribution of adult Kamchatka flounder (*Atheresthes evermanni*) in RACE-GAP summer bottom trawl surveys (upper left panel) alongside the effects of the retained habitat covariates in (lower left panels) and the probability of presence spatially predicted by the best-fitting presence–absence GAM (upper center panel). Also shown are the effects of habitat covariates retained in the best-fitting abundance (CPUE) GAM (lower right panels) and the predicted conditional abundance (CPUE where presence is predicted) across the eastern and northern Bering Sea (upper right panel). Together these figures comprise the hurdle generalized additive model (hGAM) results.

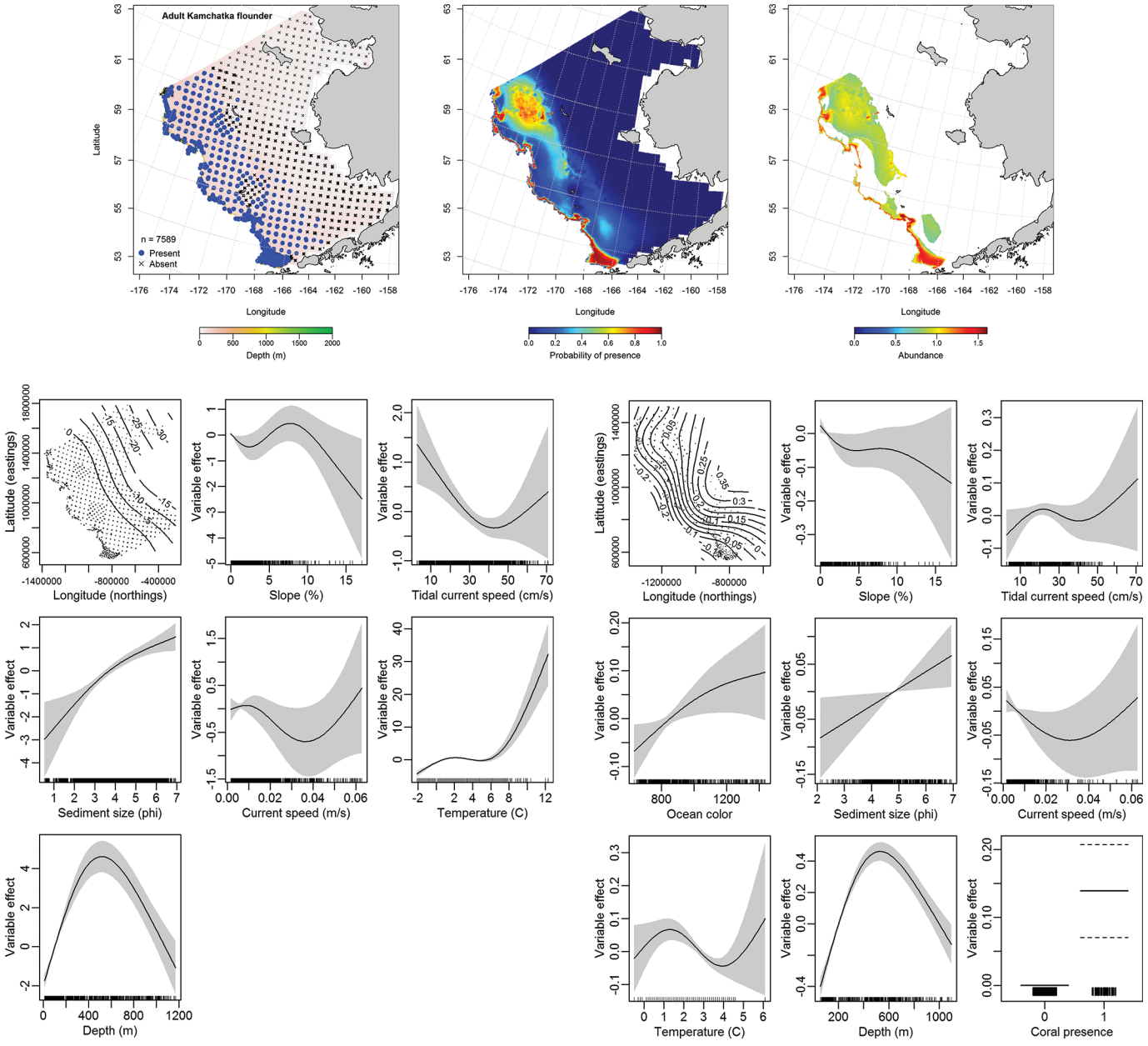

support for the utility of our SDM approach to describing EFH can be seen in the convergence between the spatial predictions from our habitat-based models and previous work showing that adult Kamchatka flounder are found along the outer shelf edge of the eastern Bering Sea in deeper waters over a relatively narrow band of bottom temperatures (Kessler 1985; Zimmermann and Goddard 1996; Mecklenburg et al. 2002).

One reason that we chose GAMs for our SDMs was to explore the relationships among habitat covariates, species distribution, and abundance. The backward stepwise term selection process we used identified the important predictors of distribution and abundance during model formulations. The eleven covariates included in the initial suite of independent predictor variables were given careful consideration to ensure that they had functional relevance to the organisms and their life stages. This is a critical step to developing robust and realistic model predictions (Elith and Leathwick 2009). Each of the covariates comprising the suite of predictors subjected to term selection represented a distinct process or habitat factor that had the potential to influence the distribution of species' life stages in the region (see Table 1 for the list and description of covariates).

When considering the more than 50 species, multiple life stages, and multiple seasons modeled in our broader study, we are able to draw general conclusions from this larger data set. Sea surface temperature was the most important determinant of egg and larval stage distribution. Bottom depth was the primary habitat covariate predicting the distribution of benthically oriented settled juvenile and adult life history stages across the eastern

Fig. 7. Seasonal distribution of Kamchatka flounder (*Atheresthes evermanni*) in commercial catches from the eastern and northern Bering Sea (left set of panels) beside model effects of habitat covariates in the maximum entropy model (MaxEnt; lower panels) followed by the spatial MaxEnt predictions of the probability of suitable Kamchatka flounder habitat (right panels).

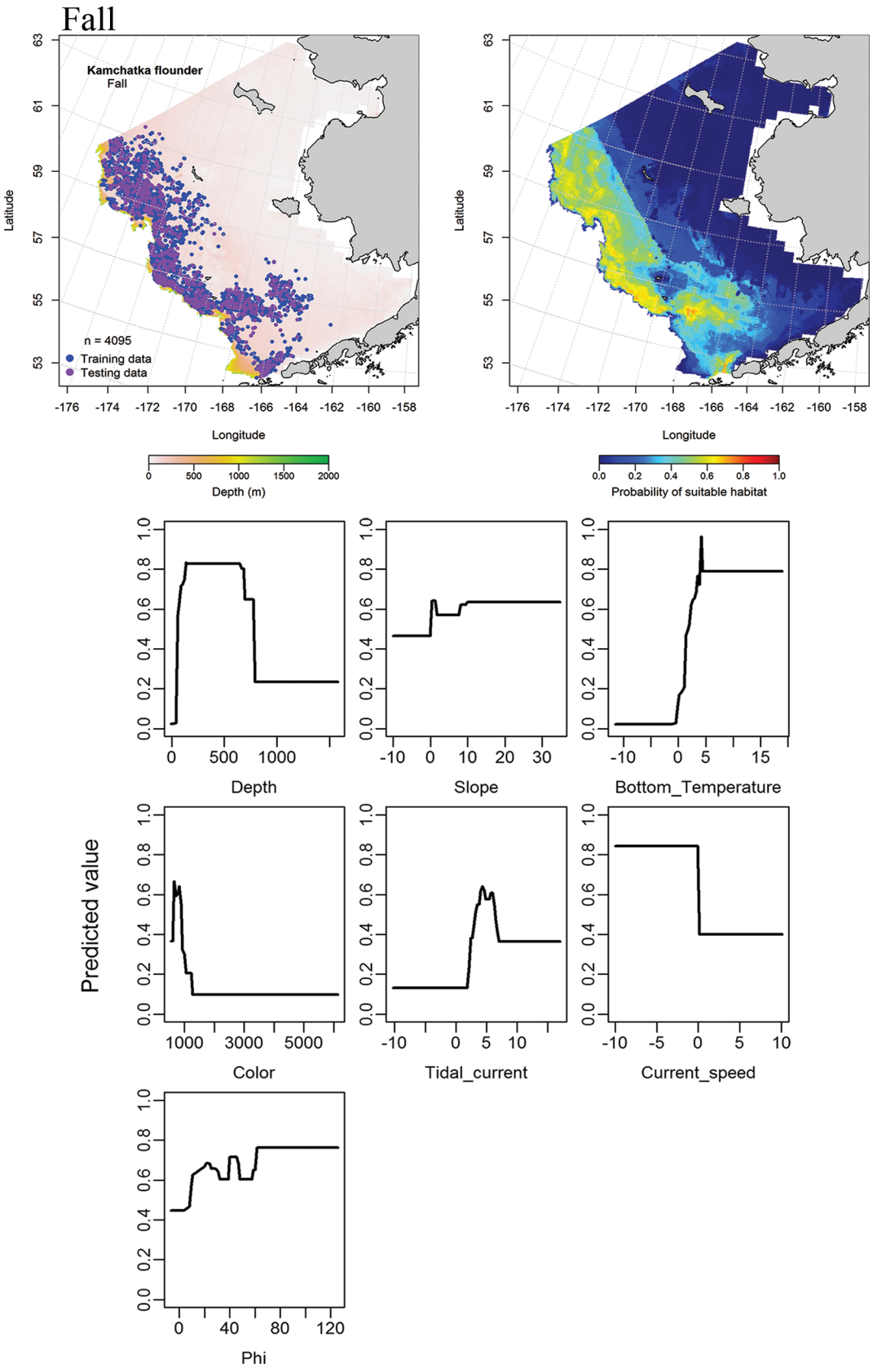

Fig. 7 (*continued*).

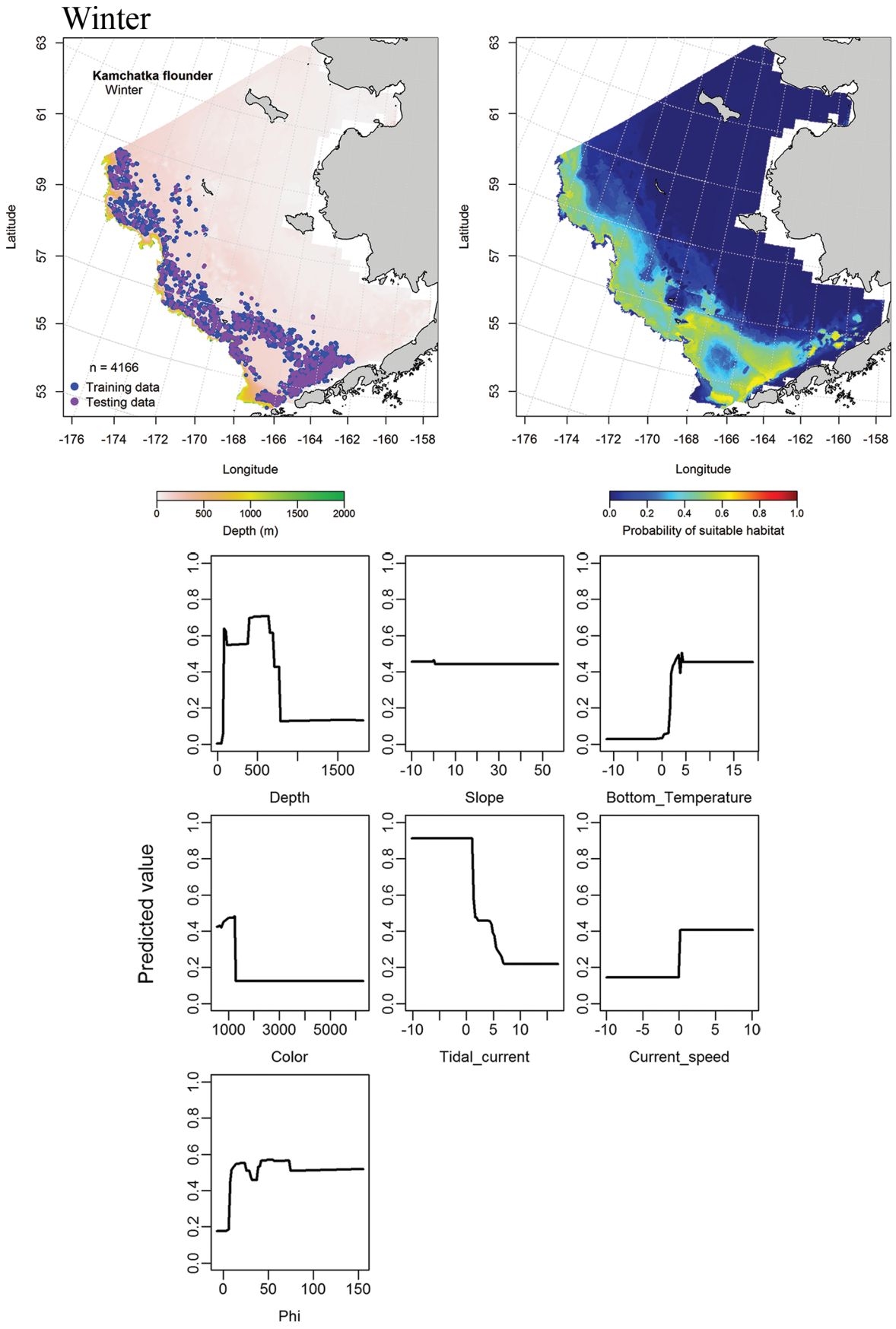

Fig. 7 (*concluded*).

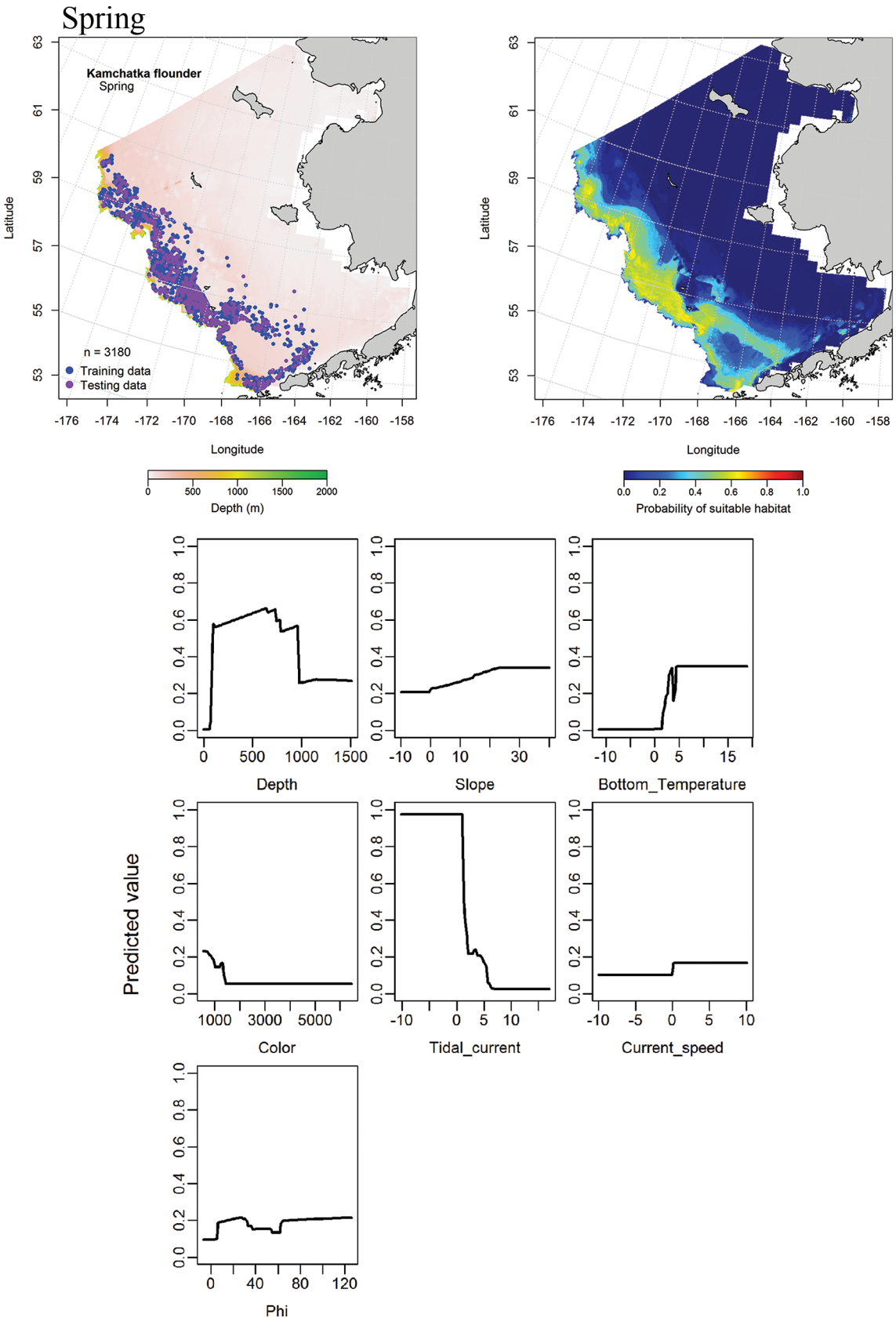

Fig. 8. Model-predicted distribution of essential fish habitat (EFH) as cumulative percentiles of the highest predictions for probability of suitable larval *Atheresthes* spp. habitat from maximum entropy (MaxEnt) modeling, abundance (CPUE) of settled Kamchatka flounder (*Atheresthes evermanni*) juveniles from the generalized additive model (GAM), conditional CPUE of adult Kamchatka flounder in summer from the hurdle GAM (hGAM), and probability of suitable Kamchatka flounder habitat from commercial catches in fall, winter, and spring (MaxEnt) across the eastern and northern Bering Sea.

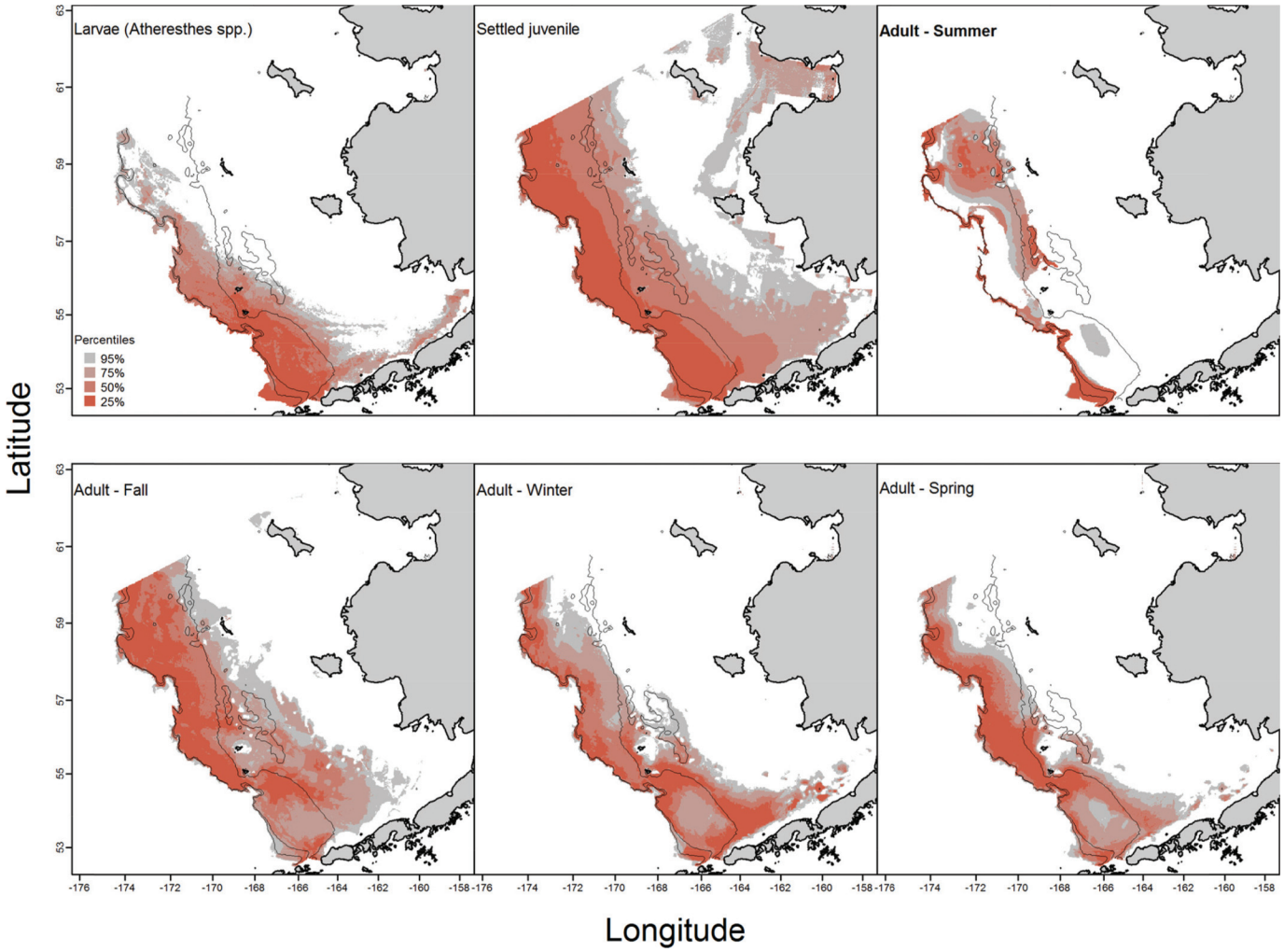

Bering Sea. In the eastern Bering Sea, predicted flatfish distributions, other than that of Kamchatka flounder and Greenland turbot, tended to be centered over shallow areas of the shelf, confirming results from other studies (McConnaughey and Smith 2000; Yeung et al. 2013). Roundfish abundance was predicted to be higher closer to the shelf break, not a surprising result considering that rockfishes tend to occur over hard substrata (Love et al. 2002). Du Preez and Tunnicliffe (2011) showed that spatial patterns of rockfish abundance were also positively influenced by the presence of biogenic structures (i.e., corals and sponges) attached to hard substrata. The other groundfishes modeled are associated with deeper water (Sigler et al. 2015). The predicted distribution and abundance of the four dominant crab species generally confirmed conclusions of previous distributional studies (e.g., Nichol and Somerton 2015; Daly et al. 2015, 2016).

Data from EcoFOCI ichthyoplankton surveys and the commercial fisheries observer program are valuable, but changing spatial coverage in the ichthyoplankton surveys and targeted effort in the commercial fisheries need to be considered when interpreting models based on these data. Since ELHS of arrowtooth and Kamchatka flounder have not historically been visually distinguished (Matarese et al. 2003; De Forest et al. 2014), ichthyoplankton records identified as *Atheresthes* spp. were used in aggregate to represent the two species of larvae. Kamchatka and arrowtooth flounder geographic distributions in the eastern Bering Sea have been shown to overlap (Zimmermann and Goddard 1996) and further justifying the aggregation of their ELHS for the SDMs.

Surveys of the eastern Bering Sea for ELHS of fishes were not spatially balanced over the course of the study period or in commercial observer data collections. Sampling effort also varied from survey to survey in terms of ichthyoplankton gear selectivity (e.g., bongo nets, neuston nets, and egg pumps were all deployed at one time or another) and targeted fishing effort. Prediction maps generated from these data may reflect changes in sampling effort and design and not necessarily the distribution of ichthyoplankton collected. For the commercial observer data, the spatial coverage of sampling and, consequently, the modeled distributions resulting from these data are highly dependent upon the target species pursued by that fishery in that season. In the Bering Sea, pollock is the most active fishery in the fall and, in recent years, has concentrated effort on the outer shelf, which is reflected in the relatively sparse observations from the inner and middle shelf during this season. Thus, Kamchatka flounder observed in commercial catches from the outer shelf in the fall were most likely reported from the pollock fleet and thus not fully representative of the spatial extent of Kamchatka flounder distribution.

Fig. 9. Predicted distribution of essential adult fish habitat for five selected flatfish species in the eastern and northern Bering Sea across four seasons. Summer distributions were predicted from RACE-GAP bottom trawl surveys using generalized additive models (GAMs) and represent the upper percentiles of abundance (CPUE), while the fall, winter, and spring distributions are predicted from commercial catch observations of presence and represent the upper percentiles of probability for suitable habitat described by maximum entropy models (MaxEnt).

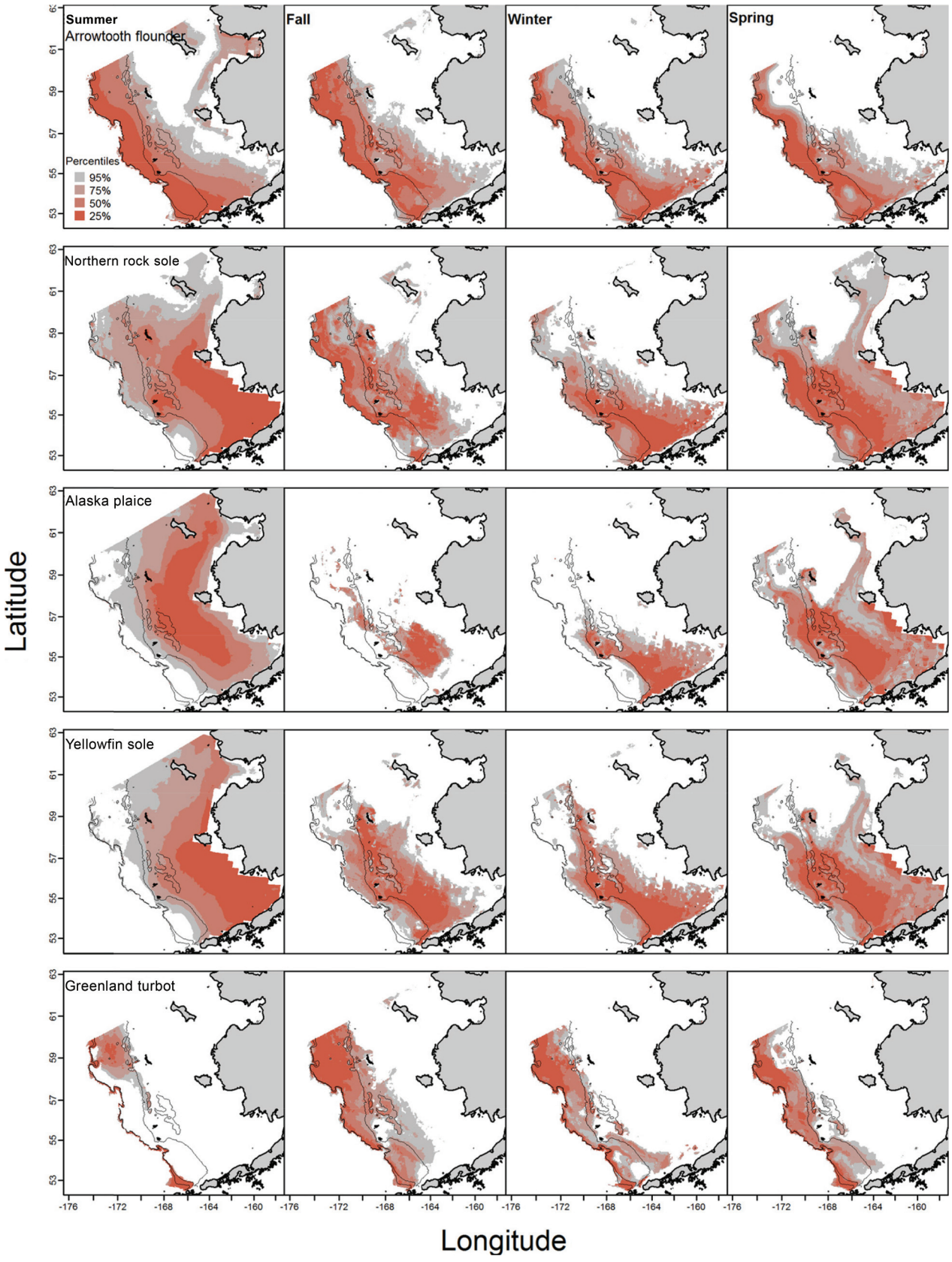

Fig. 10. Predicted distribution of essential adult fish habitat for selected roundfish and rockfish species in the eastern and northern Bering Sea across four seasons. Summer distributions were predicted from RACE-GAP bottom trawl surveys using generalized additive models (GAMs) and represent the upper percentiles of abundance (CPUE), while the fall, winter, and spring distributions are predicted from commercial catch observations of presence and represent the upper percentiles of probability for suitable habitat described by maximum entropy models (MaxEnt).

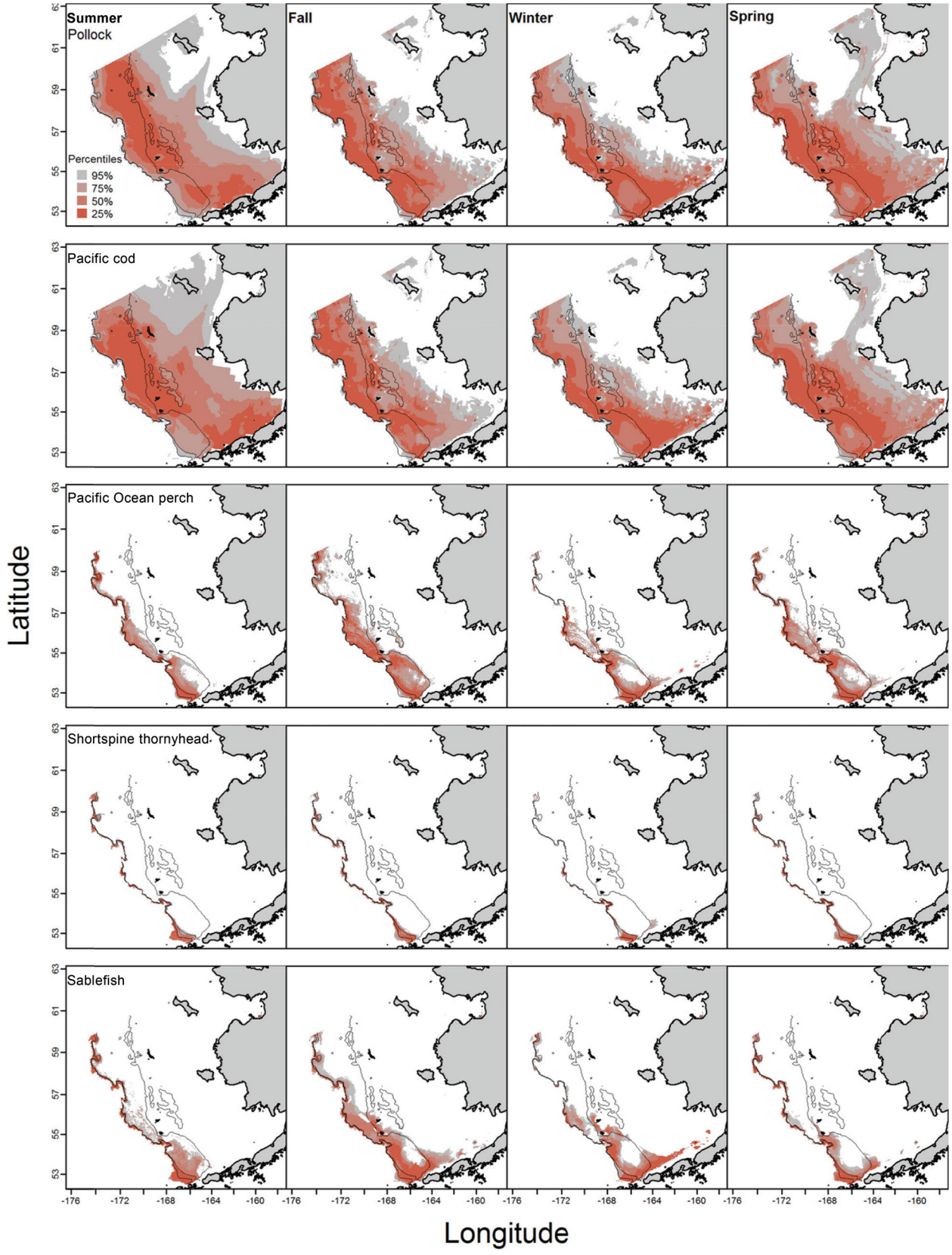

Fig. 11. Predicted distribution of essential adult habitat for four crab species in the eastern and northern Bering Sea across four seasons. Summer distributions were predicted from RACE-GAP bottom trawl surveys using generalized additive models (GAMs) and represent the upper percentiles of abundance (CPUE), while the fall, winter, and spring distributions are predicted from commercial catch observations of presence and represent the upper percentiles of probability for suitable habitat described by maximum entropy models (MaxEnt).

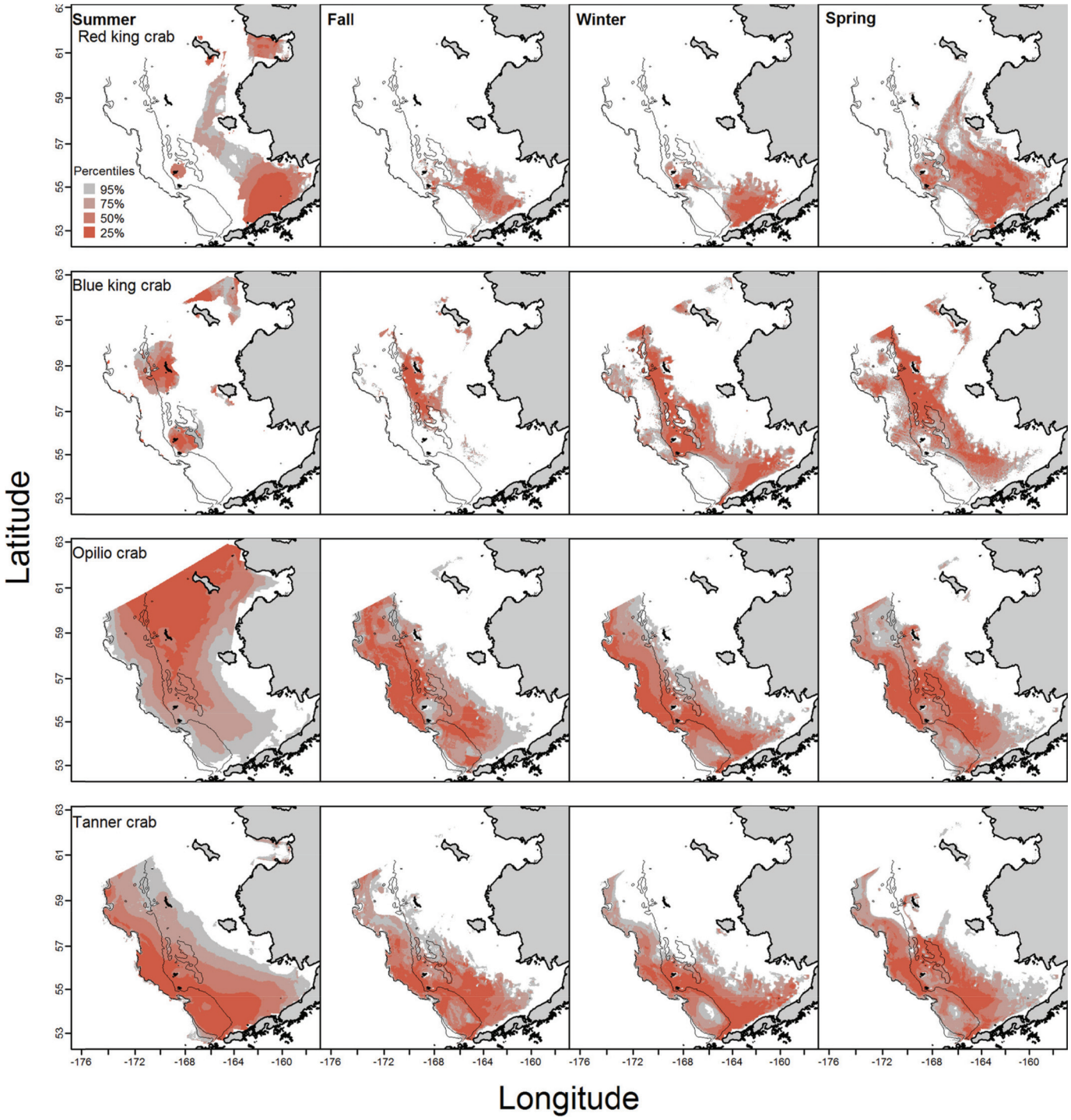

Despite these shortcomings, distributions modeled from the Eco-FOCI ichthyoplankton surveys as well as the VOE-CIA commercial fishery observations tended to confirm the shape and extent of the Kamchatka flounder distributions modeled from the systematic RACE-GAP summer bottom trawl surveys.

Because of the rigorous statistical design and the consistent year-over-year canvassing of the bottom trawl survey grid in the eastern Bering Sea, the RACE-GAP survey data are considered the best for predicting species' distribution and abundance in the region. The importance of having an underlying statistical design has been highlighted in other distribution studies (Yackulic et al. 2013), and choosing the appropriate modeling method for the type and prevalence of data available is important as well (Robinson et al. 2011; Moore et al. 2016). These and other considerations were taken in to account when deciding to employ SDMs to refine species' EFH descriptions in Alaska.

There are disadvantages to relying exclusively on SDM predictions based on the RACE-GAP bottom trawl survey data to describe EFH. For those species with distributions that vary seasonally due to spawning (Shimada and Kimura 1994; Neidetcher et al. 2014), survey coverage should include multiple times of the year and multiple years (DeLong and Collie 2004); RACE-GAP bottom trawl surveys are only conducted during the summer. In addition, interyear variability, habitat covariates that vary over short time scales (e.g., ocean productivity), or major but short-term climatological events (e.g., El Niño, storms, the "Warm Blob") can be masked when spatially and temporally integrating regional, year-over-year data sets, as we have purposely done here. Variations in the timing of spawning, ontogeny, and evolving biology of the fishes and crabs being studied can also be masked when grouping data from an area as large as the eastern Bering Sea. For example, length-at-maturity of yellowfin sole is longer in the northwest compared with the southeast eastern Bering Sea shelf (Nichol 1997), but our modeling approach combines yellowfin sole from these two areas. Rough, rocky, and untrawlable areas are not well-sampled by the RACE-GAP bottom trawl. This is especially problematic when creating area-based extrapolation of bottom trawl survey population estimates for species such as rockfishes with their predilection to occur in rocky, high-relief habitats (Cordue 2007). Our bottom trawl survey fishing gear may also be less efficient for fishes and invertebrates with behaviors or life histories that predispose them to be less available to the trawl. For example, pollock vertical distributions in the eastern Bering Sea are known to be dependent upon local water column irradiance levels such that when it is darker at depth, the pollock disperse vertically and fewer of them are available to the trawl net compared with brighter conditions when they congregate closer to the bottom (Kotwicki et al. 2009). Small fishes, flatfishes and skates, or encrusting invertebrates (e.g., corals and sponges) may be able to escape through the meshes or be passed over by the bottom trawl ground gear, altering catchability for these groups (Munro and Somerton 2001; Weinberg et al. 2002). Finally, and specific to the work detailed here, the SDM-generated patterns of distribution we used to refine EFH descriptions in Alaska are based on correlative relationships between species and their environment that do not necessarily imply functional relationships between the animals modeled and the habitat covariates retained in the formulations.

In other regions of the US, similar species distribution modeling approaches have been suggested or attempted (DeLong and Collie 2004; Moore et al. 2016). These studies have typically addressed fewer species over smaller spatial scales than we attempted in the eastern Bering Sea and yet formed the basis for our approach in the present study. Delong and Collie (2004) focused on three commercially important species in the Northwest Atlantic. They included survey year as a factor in their models to express changes in stock abundance over time and then used GAMs to describe the distribution and abundance of Atlantic cod (*Gadus morhua*), winter flounder (*Pseudopleuronectes americanus*), and yellowtail flounder (*Limanda ferruginea*) using several habitat covariates and geographic location. They successfully defined EFH for these three species using this technique and were able to apply the technique to other areas (e.g., Georges Bank). For Hawaiian deepwater snapper species, EFH was defined based on characteristics of depth, slope, and substrate using a maximum entropy model (Moore et al. 2016). Maximum entropy was found to be the best method for this data-poor group of deepwater species.

Our SDM-generated maps generally coincided with areas of concentration identified in previous descriptions of EFH for federally managed species in Alaska (NPFMC 2011, 2016*a*, 2016*b*), but differed at the margins. For instance, some areas previously ascribed to the EFH of a species now fall outside of the boundaries described by our models and vice versa. Our maps present an improvement over the previous EFH maps because they include spatially referenced levels of habitat-based distribution and abundance predictions (e.g., percentiles of abundance or probabilities of suitable habitat depicted in Figs. 8–10) that can help to identify localized hot spots (i.e., the area containing the highest 25% of abundance predictions or suitable habitat probabilities). Identifying these core habitats and having access to the other, more inclusive percentiles (e.g., top 50% and 75%) could be useful to managers and spatial planners in addition to the accepted definition for EFH of the predicted shape containing the top 95% of predictions.

Describing EFH using SDMs offers substantial advantages over less complex and more common methodologies like delineating EFH from observations of presence in fisheries-independent surveys and commercial fisheries catches. First, an SDM framework for EFH can easily incorporate new data and sources of information (DeLong and Collie 2004). Many fishery-independent surveys are conducted on a regular schedule to produce data for stock assessments. These same data can be routinely integrated into species distribution models to re-examine relationships and model fits, to validate existing models with new and independent data (e.g., Laman et al. 2015; Rooper et al. 2016), or to create new models that can be used to predict EFH from an ensemble modeling framework (e.g., Moore et al. 2016). An added benefit is that error terms and uncertainty layers can be produced as new information is incorporated with the expectation that further data will lead to refinement and better understanding of model parameters and environmental relationships.

Second, the term selection technique used with SDM identifies important relationships between presence–absence or local abundance and the environment. Specifying and parameterizing these relationships provides an opportunity to focus future research efforts on processes that have been measured (e.g., Laurel et al. 2016) or modeled (Harvey 2005; Rooper et al. 2012) and to interpret observed patterns on regional or population scales. Additionally, codifying relationships between habitat covariates and fish distribution identified with the SDM techniques demonstrated here facilitates predicting spatial shifts in fish and fisheries under changing climate regimes (e.g., Guisan and Thuiller 2005; Elith and Leathwick 2009; Kharouba et al. 2009; Reiss et al. 2011; Walsh et al. 2015) or other management scenarios (Wiens et al. 2009; Kaplan et al. 2016), a vital activity that advances ecosystem-based fisheries management. Future applications of SDM techniques with the intention of enhancing descriptions of EFH should include efforts to increase the level of information used to formulate the models, moving past distribution-based inputs and on to process-based data to more realistically depict functional ecological relationships between organisms and their environment.

The establishment of SDMs demonstrated here will facilitate the advent of reproducible quantitative analyses and risk assessments when describing EFH within management frameworks while also providing useful tools for marine spatial planning. Quantitative analysis of distribution patterns provides researchers with the opportunity to evaluate the uncertainties surrounding an EFH description. In addition, distribution maps based on different sources of data can be compared. The patterns observed from commercial fisheries in seasons besides summer did not always match the patterns predicted from summertime fisheries-independent surveys. This type of discrepancy could be used to justify additional surveys validating seasonal patterns and would improve SDMs and the EFH descriptions they support. Tools for marine spatial planning, like zonation (Moilanen et al. 2005), can incorporate spatial fish distributions, in addition to other qualitative and quantitative data layers, providing a comprehensive suite of tools that managers can use to evaluate marine ecosystems in a holistic fashion.

Understanding the spatial distribution of species is an essential step to gaining insight into ecosystem processes, informing conservation and spatial planning, and supporting the application

EBFM. The SDM approach we demonstrated here successfully met our objective to elevate the level of information used to describe EFH in Alaska marine fisheries management and will enhance EBFM in the region. For nearly all federally managed species in the three Alaska LMEs and the northern Bering Sea, we were able to increase the information level input when creating the new descriptions of EFH. In most cases, we were able to predict species distribution from habitat-specific density data (Level 2 information). However, we anticipate a future challenge as spatial definitions of EFH like these become more integrated into EBFM. A likely result will be greater overlap of EFH among multiple species and life stages. This will present new issues for resource managers to address when more points on the map come to represent EFH for many species' life stages.

An application for the SDMs that is becoming more common is to forecast shifts in spatial distributions under changing climate regimes (e.g., Guisan and Thuiller 2005; Elith and Leathwick 2009; Kharouba et al. 2009; Reiss et al. 2011; Walsh et al. 2015). Changing thermal regimes have the potential to impact a species' life history and distribution. For instance, parturition timing changes could lead to spatially linked ontogenetic stages becoming disconnected in space and time, or the opposite could occur (spatial overlap for species' life stages could increase, leading to greater competition for resources or density dependence). Forecasting exercises using SDMs could help inform long-range planning for EBFM. The SDMs we have established here can also be used to hindcast species' distributions using past survey data that could both act as a form of model validation and determine if distributional shifts have occurred in the past. Certainly, thermal regimes have varied over the years, but caution would have to be exercised, since survey technology has evolved over the same time frame, and the impact of active fisheries over those intervening years cannot be overlooked.

Acknowledgements

The authors are grateful to Megan Prescott for her diligence and work on the bathymetry layers for each region. This project was funded by the Alaska Fisheries Science Center – Alaska Regional Office (AKRO) Habitat Research Program. We thank John V. Olson and Steve Lewis in AKRO for providing the data from the Alaska fisheries observer program. We thank Al Hermann for providing ROMS model outputs. We thank all of the vessel companies, ship's crews, sea-going scientists, and observers who collected these data. Finally, the authors are grateful to the Alaska Fisheries Science Center reviewers Kathy Mier, Wayne Palsson, Jeff Napp, and James Lee, as well as two anonymous reviewers, all of whose comments and suggested revisions greatly improved this manuscript.

References

Alverson, D.L., and Pereyra, W.T. 1969. Demersal fish explorations in the northeastern Pacific Ocean — an evaluation of exploratory fishing methods and analytical approaches to stock size and yield forecasts. J. Fish. Res. Board Can. **26**: 1985–2001. doi:10.1139/f69-188.

Barry, S.C., and Welsh, A.H. 2002. Generalized additive modelling and zero inflated count data. Ecol. Mod. **157**(2–3): 179–188. doi:10.1016/S0304-3800(02)00194-1.

Behrenfeld, M.J., and Falkowski, P.G. 1997. Photosynthetic rates derived from satellite chorlophyll concentration. Limnol. Oceanogr. **42**(1): 1–20. doi:10.4319/lo.1997.42.1.0001.

Brodeur, R.D. 2001. Habitat-specific distribution of Pacific ocean perch (*Sebastes alutus*) in Pribilof Canyon, Bering Sea. Cont. Shelf Res. **21**(3): 207–224. doi:10.1016/S0278-4343(00)00083-2.

Buckley, T.W., Greig, A., and Boldt, J.L. 2009. Describing summer pelagic habitat over the continental shelf in the eastern Bering Sea, 1982–2006. NOAA Tech. Memo. NMFS-AFSC-196 [online]. Available from http://www.afsc.noaa.gov/Publications/AFSC-TM/NOAA-TM-AFSC-196.pdf [accessed 22 March 2017].

Chambers, J., and Hastie, T. 1992. Statistical models in S. Wadsworth and Brooks/Cole, Pacific Grove, California.

Coachman, L.K. 1986. Circulation, water masses, and fluxes on the southeastern Bering Sea shelf. Cont. Shelf Res. **5**(1–2): 23–108. doi:10.1016/0278-4343(86)90011-7.

Cordue, P.L. 2007. A note on non-random error structure in trawl survey abundance indices. ICES J. Mar. Sci. **64**: 1333–1337. doi:10.1093/icesjms/fsm134.

Cragg, J.G. 1971. Some statistical models for limited dependent variables with application to the demand for durable goods. Econometrica, **39**: 829–844. doi:10.2307/1909582.

Daly, B.J., Armistead, C.E., and Foy, R.J. 2015. The 2015 eastern Bering Sea continental shelf bottom trawl survey: results for commercial crab. US Dep. Commer., NOAA Tech. Memo. NMFS-AFSC-308 [online]. Available from http://www.afsc.noaa.gov/Publications/AFSC-TM/NOAA-TM-AFSC-308.pdf [accessed 22 March 2017].

Daly, B.J., Armistead, C.E., and Foy, R.J. 2016. The 2016 eastern Bering Sea continental shelf bottom trawl survey: results for commercial crab. US Dep. Commer., NOAA Tech. Memo. NMFS-AFSC-327 [online]. Available from http://www.afsc.noaa.gov/Publications/AFSC-TM/NOAA-TM-AFSC-327.pdf [accessed 22 March 2017].

Danielson, S., Curchitser, E., Hedstrom, K., Weingartner, T., and Stabeno, P. 2011. On ocean and sea ice modes of variability in the Bering Sea. J. Geophys. Res. **116**: C12034. doi:10.1029/2011JC007389.

De Forest, L., Duffy-Anderson, J.T., Heintz, R.A., Matarese, A.C., Siddon, E.C., Smart, T.I., and Spies, I.B. 2014. Taxonomy of the early life stages of arrowtooth flounder (*Atheresthes stomias*) and Kamchatka flounder (*A. evermanni*) in the eastern Bering Sea, with notes on distribution and condition. Deep-Sea Res. Part II Top. Stud. Oceanogr. **109**: 181–189. doi:10.1016/j.dsr2.2014.05.005.

DeLong, A.K., and Collie, J.S. 2004. Defining essential fish habitat: a model-based approach. Rhode Island Sea Grant, Narragansett, Rhode Island.

DeLong, E.R., DeLong, D.M., and Clarke-Pearson, D.L. 1988. Comparing the areas under two or more correlated receiver operating characteristic curves: a nonparametric approach. Biometrics, **44**(3): 837–845. doi:10.2307/2531595. PMID:3203132.

Denis, V., Lejeunem, J., and Robin, J.P. 2002. Spatio-temporal analysis of commercial trawler data using general additive models: patterns of Loliginid squid abundance in the north-east Atlantic. ICES J. Mar. Sci. **59**(3): 633–648. doi:10.1006/jmsc.2001.1178.

Du Preez, C., and Tunnicliffe, V. 2011. Shortspine thornyhead and rockfish (Scorpaenidae) distribution in response to substratum, biogenic structures and trawling. Mar. Ecol. Prog. Ser. **425**: 217–231. doi:10.3354/meps09005.

Egbert, G.D., and Erofeeva, S.Y. 2002. Efficient inverse modeling of barotropic ocean tides. J. Atmosph. Ocean. Technol. **19**(2): 183–204. doi:10.1175/1520-0426(2002)019<0183:EIMOBO>2.0.CO;2.

Elith, J., and Leathwick, J.R. 2009. Species distribution models: Ecological explanation and prediction across space and time. Annu. Rev. Ecol. Evol. Syst. **40**: 677–697. doi:10.1146/annurev.ecolsys.110308.120159.

Elith, J., Phillips, S.J., Hastie, T., Dudik, M., Chee, Y.E., and Yates, C.J. 2011. A statistical explanation of MaxEnt for ecologists. Diversity Distrib. **17**(1): 43–57. doi:10.1111/j.1472-4642.2010.00725.x.

Essential Fish Habitat Final Rule 50. 2002. U.S. CFR 600.815(a)(1)(iii)(A)(1)-(4).

Federal Register. 2010. Executive Order 13547 — Stewardship of the Ocean, Our Coasts, and the Great Lakes [online]. Available from https://energy.gov/sites/prod/files/nepapub/nepa_documents/RedDont/Req-EO13547watersteward.pdf.

Freeman, E. 2010. Presence–Absence model evaluation: package 'PresenceAbsence' version 1.1.5 (R, v3.0.1).

Grebmeier, J.M., McRoy, C.P., and Feder, H.M. 1988. Pelagic–benthic coupling on the shelf of the northern Bering and Chukchi Seas. I. Food supply source and benthic biomass. Mar. Ecol. Prog. Ser. **48**: 57–67. doi:10.3354/meps048057.

Guisan, A., and Thuiller, W. 2005. Predicting species distribution: offering more than simple habitat models. Ecol. Lett. **8**(9): 993–1009. doi:10.1111/j.1461-0248.2005.00792.x.

Harvey, C.J. 2005. Effects of El Niño events on energy demand and egg production of rockfish (Scorpaenidae: *Sebastes*): a bioenergetics approach. Fish. Bull. **103**: 71–83.

Hastie, T.J., and Tibshirani, R.J. 1986. Generalized additive models. Stat. Sci. **1**(3): 297–318. doi:10.1214/ss/1177013604.

Hastie, T.J., and Tibshirani, R.J. 1990. Generalized additive models. Monogr. Stat. Appl. Prob. 43.

Hegland, T.J., Raakjaer, J., and van Tatenhove, J. 2015. Implementing ecosystem-based marine management as a process of regionalization: Some lessons from the Baltic Sea. Ocean Coast. Manage. **117**: 14–22. doi:10.1016/j.ocecoaman.2015.08.005.

Heifetz, J., Wing, B.L., Stone, R., Malecha, P., and Courtney, D. 2005. Corals of the Aleutian Islands. Fish. Oceanogr. **14**(s1): 131–138. doi:10.1111/j.1365-2419.2005.00371.x.

Hernandez-Delgado, E.A., and Sabat, A.M. 2000. Ecological status of essential fish habitats through an anthropogenic environmental stress gradient in Puerto Rican coral reefs. Proc. Gulf Carib. Fish. Inst. **51**: 457–470.

Hijams, R.J., Phillips, S., Leathwick, J., and Elith, J. 2014. Species distribution modeling: package 'dismo' version 1.0-5 (R v3.0.1).

Hijmans, R.J., van Etten, J., Mattiuzzi, M., Sumner, M., Greenberg, J.A., Lamigueiro, O.P., Bevan, A., Racine, E.B., and Shortridge, A. 2015. Geographic data analysis and modeling: package 'raster', version 2.3-24 (R v3.0.1).

Hoff, G.R. 2013. Results of the 2012 eastern Bering Sea upper continental slope survey of groundfish and invertebrate resources. US Dep. Commer., NOAA Tech. Memo. NMFS-AFSC-258 [online]. Available from http://www.afsc.noaa.gov/Publications/AFSC-TM/NOAA-TM-AFSC-258.pdf [accessed 20 March 2017].

Hoff, G.R., and Britt, L.L. 2011. Results of the 2010 eastern Bering Sea upper continental slope survey of groundfish and invertebrate resources. US Dep.

Commer., NOAA Tech. Memo. NMFS-AFSC-224 [online]. Available from http://www.afsc.noaa.gov/Publications/AFSC-TM/NOAA-TM-AFSC-224.pdf [accessed 20 March 2017].

Hosmer, D.W., and Lemeshow, S. 2005. Multiple logistic regression. 2nd ed. John Wiley and Sons, Hoboken, N.J.

Ichthyoplankton Information System. 2016. [11 October 2016.] National Oceanic and Atmospheric Administration [online]. Available from http://access.afsc.noaa.gov/ichthyo/index.php [accessed 26 September 2017].

Kaplan, I.C., Williams, G.D., Bond, N.A., Hermann, A.J., and Siedlecki, S.A. 2016. Cloudy with a chance of sardines: forecasting sardine distributions using regional climate models. Fish. Oceanogr. **25**(1): 15–27. doi:10.1111/fog.12131.

Kessler, D.W. 1985. Alaska's saltwater fishes and other sea life: a field guide. Alaska Northwest Publishing Company. Anchorage, Alaska.

Kharouba, H.M., Algar, A.C., and Kerr, J.T. 2009. Historically calibrated predictions of butterfly species' range shift using global change as a pseudo-experiment. Ecol. **90**(8): 2213–2222. doi:10.1890/08-1304.1.

Kotwicki, S., De Robertis, A., von Szalay, P., and Towler, R. 2009. The effect of light intensity on the availability of walleye pollock (*Theragra chalcogramma*) to bottom trawl and acoustic surveys. Can. J. Fish. Aquat. Sci. **66**(6): 983–994. doi:10.1139/F09-055.

Kumar, S., and Stohlgren, T.J. 2009. Maxent modeling for predicting suitable habitat for threatened and endangered tree *Canacomyrica monticola* in New Caledonia. J. Ecol. Nat. Environ. **1**(4): 94–98.

Laman, E.A., Kotwicki, S., and Rooper, C.N. 2015. Correlating environmental and biogenic factors with abundance and distribution of Pacific ocean perch (*Sebastes alutus*) in the Aleutian Islands, Alaska. Fish. Bull. **113**(3): 270–289. doi:10.7755/FB.113.3.4.

Laman, E.A., Rooper, C.N., Turner, K., Rooney, S., Cooper, D.W., and Zimmermann, M. 2017. Model-based essential fish habitat definitions for Bering Sea groundfish species. US Dep. Commer., NOAA Tech. Memo. NMFS-AFSC-357. doi:10.7289/V5/TM-AFSC-357.

Laurel, B.J., Spencer, M., Iseri, P., and Copeman, L.A. 2016. Temperature-dependent growth and behavior of juvenile Arctic cod (*Boreogadus saida*) and co-occurring North Pacific gadids. Polar Biol. **39**(6): 1127–1135. doi:10.1007/s00300-015-1761-5.

Lauth, R.R. 2011. Results of the 2010 eastern and northern Bering Sea continental shelf bottom trawl survey of groundfish and invertebrate fauna. US Dep. Commer., NOAA Tech. Memo. NMFS-AFSC-227 [online]. Available from http://www.afsc.noaa.gov/Publications/AFSC-TM/NOAA-TM-AFSC-227.pdf [accessed 20 March 2017].

Lauth, R.R., and Conner, J. 2014. Results of the 2011 Eastern Bering Sea continental shelf bottom trawl survey of groundfish and invertebrate fauna. US Dep. Commer., NOAA Tech. Memo. NMFS-AFSC-266 [online]. Available from http://www.afsc.noaa.gov/Publications/AFSC-TM/NOAA-TM-AFSC-266.pdf [accessed 20 March 2017].

Love, M.S., Yoklavich, M., and Thorsteinson, L. 2002. The Rockfishes of the Northeast Pacific. University of California Press, London.

Magnuson–Stevens Fishery Conservation and Management Act. 1996. Public Law 94-265 [online]. Available from http://www.nmfs.noaa.gov/sfa/magact/ [accessed 15 November 2016].

Malecha, P.W., Stone, R.P., and Heifetz, J. 2005. Living substrate in Alaska: Distribution, abundance, and species associations. *In* Benthic habitats and the effects of fishing. *Edited by* P.W. Barnes and J.P. Thomas. Am. Fish. Soc. Symp. 41, Bethesda, Md. pp. 289–299.

Manel, S., Ceri Williams, H., and Ormerod, S.J. 2001. Evaluating presence–absence models in ecology: the need to account for prevalence. J. Appl. Ecol. **38**(5): 921–931. doi:10.1046/j.1365-2664.2001.00647.x.

Marliave, J., and Challenger, W. 2009. Monitoring and evaluating rockfish conservation areas in British Columbia. Can. J. Fish. Aquat. Sci. **66**(6): 995–1006. doi:10.1139/F09-056.

Matarese, A.C., Blood, D.M., Picquelle, S.J., and Benson, J.L. 2003. Atlas of abundance and distribution patterns of ichthyoplankton from the northeast Pacific Ocean and Bering Sea ecosystems based on research conducted by the Alaska Fisheries Science Center (1972–1996). NOAA Prof. Paper NMFS 1 [online]. Available from http://spo.nwr.noaa.gov/pp1.pdf [accessed 10 April 2017].

McConnaughey, R.A., and Smith, K.R. 2000. Associations between flatfish abundance and surficial sediments in the eastern Bering Sea. Can. J. Fish. Aquat. Sci. **57**(12): 2410–2419. doi:10.1139/f00-219.

Mecklenburg, C.W., Mecklenburg, T.A., and Thorsteinson, L.K. 2002. Fishes of Alaska. American Fisheries Society, Bethesda, Md.

Metcalf, S.J., Gaughan, D.J., and Shaw, J. 2009. Conceptual models for ecosystem based fisheries management (EBFM) in Western Australia. Fish. Res. Rept. No. 194 [online]. URL: http://researchrepository.murdoch.edu.au/id/eprint/17591/ [accessed 11 April 2017].

Moilanen, A., Franco, A.M.A., Early, R., Fox, R., Wintle, B., and Thomas, C.D. 2005. Prioritizing multiple-use landscapes for conservation: methods for large multi-species planning problems. Proc. R. Soc. B Biol. Sci. **272**(1575): 1885–1891. doi:10.1098/rspb.2005.3164.

Moore, C.H., Harvey, E.S., and Van Niel, K.P. 2009. Spatial prediction of demersal fish distributions: enhancing our understanding of species–environment relationships. ICES J. Mar. Sci. **66**(9): 2068–2075. doi:10.1093/icesjms/fsp205.

Moore, C., Drazen, J.C., Radford, B.T., Kelley, C., and Newman, S.J. 2016. Improving essential fish habitat designation to support sustainable ecosystem-based fisheries management. Mar. Pol. **69**: 32–41. doi:10.1016/j.marpol.2016.03.021.

Munro, P.T., and Somerton, D.A. 2001. Maximum likelihood and non-parametric methods for estimating trawl footrope selectivity. ICES J. Mar. Sci. **58**(1): 220–229. doi:10.1006/jmsc.2000.1004.

NMFS. 2010. Marine fisheries habitat assessment improvement plan. Report of the National Marine Fisheries Service Habitat Assessment Improvement Plan Team. US Dep. Commer., NOAA Tech. Memo. NMFS-F/SPO-108.

Neidetcher, S.K., Hurst, T.P., Ciannelli, L., and Logerwell, E.A. 2014. Spawning phenology and geography of Aleutian Islands and eastern Bering Sea Pacific cod (*Gadus macrocephalus*). Deep-Sea Res. Part II Top. Stud. Oceanogr. **109**: 204–214. doi:10.1016/j.dsr2.2013.12.006.

Nichol, D.G. 1997. Effects of geography and bathymetry on growth and maturity of yellowfin sole, *Pleuronectes asper*, in the eastern Bering Sea. Fish. Bull. **95**(3): 494–503.

Nichol, D.G., and Somerton, D.A. 2015. Seasonal migrations of morphometrically mature male snow crab (*Chionoecetes opilio*) in the eastern Bering Sea in relation to mating dynamics. Fish. Bull. **113**(3): 313–326. doi:10.7755/FB.113.3.7.

NPFMC. 2011. Fishery Management Plan for Bering Sea/Aleutian Islands King and Tanner Crabs [online]. North Pacific Fisheries Management Council, 605 W. 4th Ave. Ste. 306, Anchorage AK 99501, USA. Available from http://www.npfmc.org/wp-content/PDFdocuments/fmp/CrabFMPOct11.pdf#page=1 [accessed 15 November 2016].

NPFMC. 2016*a*. Fishery Management Plan for Groundfish of the Gulf of Alaska [online]. North Pacific Fisheries Management Council, 605 W. 4th Ave. Ste. 306, Anchorage AK 99501, USA. Available from http://www.npfmc.org/wp-content/PDFdocuments/fmp/GOA/GOAfmp.pdf#page=1 [accessed 15 November 2016].

NPFMC. 2016*b*. Fishery Management Plan for Groundfish of the Bering Sea and Aleutian Islands Management Area [online]. North Pacific Fisheries Management Council, 605 W. 4th Ave. Ste. 306, Anchorage AK 99501, USA. Available from http://www.npfmc.org/wp-content/PDFdocuments/fmp/BSAI/BSAIfmp.pdf#page=1 [accessed 15 November 2016].

Phillips, S.J., Anderson, R.P., and Schapire, R.E. 2006. Maximum entropy modeling of species geographic distributions. Ecol. Model. **190**(3–4): 231–259. doi:10.1016/j.ecolmodel.2005.03.026.

Pikitch, E.K., Santora, C., Babcock, E.A., Bakun, A., Bonfil, R., Conover, D.O., Dayton, P., Doukakis, P., Fluharty, D., Heneman, B., Houde, E.D., Link, J., Livingston, P.A., Mangel, M., McAllister, M.K., Pope, J., and Sainsbury, K.J. 2004. Ecosystem-based fishery management. Science, **305**(5682): 346–347. doi:10.1126/science.1098222.

Politou, C.Y., Tserpes, G., and Dokos, J. 2008. Identification of deep-water pink shrimp abundance distribution patterns and nursery grounds in the eastern Mediterranean by means of generalized additive modeling. Hydrobiologia, **612**(1): 99–107. doi:10.1007/s10750-008-9488-8.

Potts, J., and Elith, J. 2006. Comparing species abundance models. Ecol. Model. **199**: 153–163. doi:10.1016/j.ecolmodel.2006.05.025.

R Core Team. 2013. R: a language and environment for statistical computing [online]. R Foundation for Statistical Computing, Vienna, Austria. Available from http://www.R-project.org/.

Reiss, H., Cunze, S., König, K., Neumann, H., and Kröncke, I. 2011. Species distribution modelling of marine benthos: a North Sea case study. Mar. Ecol. Prog. Ser. **442**: 71–86. doi:10.3354/meps09391.

Robinson, L.M., Elith, J., Hobday, A.J., Pearson, R.G., Kendall, B.E., Possingham, H.P., and Richardson, A.J. 2011. Pushing the limits in marine species distribution modelling: lessons from the land present challenges and opportunities. Glob. Ecol. Biogeogr. **20**(6): 789–802. doi:10.1111/j.1466-8238.2010.00636.x.

Rooper, C.N., Hoff, G.R., and DeRobertis, A. 2010. Assessing habitat utilization and rockfish (*Sebastes* spp.) biomass on an isolated rocky ridge using acoustics and stereo image analysis. Can. J. Fish. Aquat. Sci. **67**(10): 1658–1670. doi:10.1139/F10-088.

Rooper, C.N., Boldt, J.L., Batten, S.D., and Gburski, C. 2012. Growth and production of Pacific ocean perch (*Sebastes alutus*) in nursery habitats of the Gulf of Alaska. Fish. Oceangr. **21**(6): 415–429. doi:10.1111/j.1365-2419.2012.00635.x.

Rooper, C.N., Zimmermann, M., Prescott, M.M., and Hermann, A.J. 2014. Predictive models of coral and sponge distribution, abundance, and diversity in bottom trawl surveys of the Aleutian Islands, Alaska. Mar. Ecol. Prog. Ser. **503**: 157–176. doi:10.3354/meps10710.

Rooper, C.N., Sigler, M.F., Goddard, P., Malecha, P., Towler, R., Williams, K., Wilborn, R., and Zimmermann, M. 2016. Validation and improvement of species distribution models for structure-forming invertebrates in the eastern Bering Sea with an independent survey. Mar. Ecol. Prog. Ser. **551**: 117–130. doi:10.3354/meps11703.

Rooper, C.N., Zimmermann, M., and Prescott, M.M. 2017. Comparison of modeling methods to predict the spatial distribution of deep-sea coral and sponge in the Gulf of Alaska. Deep-Sea Res. Part I Oceanogr. Res. Pap. **126**: 148–161. doi:10.1016/j.dsr.2017.07.002.

Rosenberg, A., Bigford, T.E., Leathery, S., Hill, R.L., and Bickers, K. 2000. Ecosystem approaches to fishery management through essential fish habitat. Bull. Mar. Sci. **66**(3): 535–542.

Sheehan, K.L., Esswein, S.T., Dorr, B.S., Yarrow, G.K., and Johnson, R.J. 2017. Using species distribution models to define nesting habitat of the eastern metapopulation of double-crested cormorants. Ecol. Evol. **7**(1): 409–418. doi:10.1002/ece3.2620. PMID:28070303.

Shelton, P.A. 2007. The weakening role of science in the management of ground-

fish off the east coast of Canada. ICES J. Mar. Sci. **64**(4): 723–729. doi:10.1093/icesjms/fsm008.

Shimada, A.M., and Kimura, D.K. 1994. Seasonal movements of Pacific cod, *Gadus macrocephalus*, in the eastern Bering Sea and adjacent waters based on tag–recapture data. Fish. Bull. **92**(4): 800–816.

Sigler, M.F., Cameron, M.F., Eagleton, M.P., Faunce, C.H., Heifetz, J., Helser, T.E., Laurel, B.J., Lindeberg, M.R., McConnaughey, R.A., Ryer, C.H., and Wilderbuer, T.K. 2012. Alaska Essential Fish Habitat Research Plan: a research plan for the National Marine Fisheries Service's Alaska Fisheries Science Center and Alaska Regional Office. AFSC Processed Rep. 2012-06 [online]. Available from http://www.afsc.noaa.gov/Publications/ProcRpt/PR2012-06.pdf [accessed 23 March 2017].

Sigler, M.F., Rooper, C.N., Hoff, G.R., Stone, R.P., McConnaughey, R.A., and Wilderbuer, T.K. 2015. Faunal features of submarine canyons on the eastern Bering Sea slope. Mar. Ecol. Prog. Ser. **526**: 21–40. doi:10.3354/meps11201.

Smith, K.R., and McConnaughey, R.A. 1999. Surficial sediments of the eastern Bering Sea continental shelf: EBSSED database documentation. US Dep. Commer., NOAA Tech. Memo. NMFS-AFSC-104 [online]. Available from http://www.afsc.noaa.gov/Publications/AFSC-TM/NOAA-TM-AFSC-104.pdf [accessed 23 March 2017].

Stal, J., Leif, P., and Wennhage, H. 2007. Food utilization by coastal fish assemblages in rocky and soft bottoms on the Swedish west coast: inference for identification of essential fish habitats. Estuar. Coast. Shelf Sci. **71**(3–4): 593–607. doi:10.1016/j.ecss.2006.09.008.

Stark, J.W. 2012. Female maturity, reproductive potential, relative distribution, and growth compared between arrowtooth flounder (*Atheresthes stomias*) and Kamchatka flounder (*A. evermanni*) indicating concerns for management. J. Appl. Ichthyol. **28**(2): 226–230. doi:10.1111/j.1439-0426.2011.01885.x.

Stone, R., Lehnert, H., and Reiswig, H. 2011. A guide to the deep-water sponges of the Aleutian Island Archipelago. NOAA Professional Paper NMFS 12 [online]. Available from http://spo.nwr.noaa.gov/pp12.pdf [accessed 23 March 2017].

Swartzman, G., Huang, C., and Kaluzny, S. 1992. Spatial analysis of Bering Sea groundfish survey data using generalized additive models. Can. J. Fish. Aquat. Sci. **49**(7): 1366–1378. doi:10.1139/f92-152.

Turner, K., Rooper, C.N., Laman, E.(A.), Rooney, S., Cooper, D.W., and Zimmermann, M. 2017. Model-based essential fish habitat definitions for Aleutian Islands groundfish species. US Dep. Commer., NOAA Tech. Memo. NMFS-AFSC-360. doi:10.7289/V5/TM-AFSC-360.

Venables, W.N., and Ripley, B.D. 2002. Modern applied statistics with S. 4th ed. Springer Science+Business Media, New York.

Wakabayashi, K., Bakkala, R.G., and Alton, M.S. 1985. Methods of the Japan demersal trawl surveys. *In* Results of cooperative:- Japan groundfish investigations in the Bering Sea during May–August 1979. *Edited by* R.G. Bakkala and K. Wakabayashi. Int. N. Pac. Fish. Comm. Bull. 44. pp. 7–29.

Walsh, H.J., Richardson, D.E., Marancik, K.E., and Hare, J.A. 2015. Long-term changes in the distributions of larval and adult fish in the Northeast U.S. Shelf Ecosystem. PLoS ONE, **10**(9): e0137382. doi:10.1371/journal.pone.0137382. PMID:26398900.

Watson, D.F., and Philip, G.M. 1985. A refinement of inverse distance weighted interpolation. Geo-Processing, **2**(4): 315–327.

Weinberg, K.L., and Kotwicki, S. 2008. Factors influencing net width and sea floor contact of a survey bottom trawl. Fish. Res. **93**(3): 265–279. doi:10.1016/j.fishres.2008.05.011.

Weinberg, K.L., Somerton, D.A., and Munro, P.T. 2002. The effect of trawl speed on the footrope capture efficiency of a survey trawl. Fish. Res. **58**(3): 303–313. doi:10.1016/S0165-7836(01)00395-2.

Wiens, J.A., Stralberg, D., Jongsomjit, D., Howell, C.A., and Snyder, M.A. Niches, models, and climate change: assessing the assumptions and uncertainties. Proc. Natl. Acad. Sci. U.S.A. **106**(S2): 19729–19736. doi:10.1073/pnas.0901639106. PMID:19822750.

Wilson, K.A., Westphal, M.I., Possingham, H.P., and Elith, J. 2005. Sensitivity of conservation planning to different approaches to using predicted species distribution data. Biol. Conserv. **122**(1): 99–112. doi:10.1016/j.biocon.2004.07.004.

Wood, S.N. 2006. Generalized additive models: an introduction with R. Chapman and Hall/CRC, Boca Raton, Fla.

Wood, S.N. 2014. Mixed GAM computation vehicle with GCV/AIC/REML smoothness estimation: package 'mgcv' version 1.8-4 (R, v3.0.1).

Yackulic, C.B., Chandler, R., Zipkin, E.F., Royle, J.A., Nichols, J.D., Campbell Grant, E.H., and Veran, S. 2013. Presence-only modelling using MAXENT: when can we trust the inferences? Methods Ecol. Evol. **4**(3): 236–243. doi:10.1111/2041-210x.12004.

Yeung, C., Yang, M.S., Jewett, S.C., and Naidu, A.S. 2013. Polychaete assemblage as surrogate for prey availability in assessing southeastern Bering Sea flatfish habitat. J. Sea Res. **76**: 211–221. doi:10.1016/j.seares.2012.09.008.

Zimmermann, M., and Benson, J.L. 2013. Smooth sheets: How to work with them in a GIS to derive bathymetry, features and substrates. NOAA Tech. Memo. NMFS-AFSC-249 [online]. Available from http://www.afsc.noaa.gov/Publications/AFSC-TM/NOAA-TM-AFSC-249.pdf [accessed 10 April 2017).

Zimmermann, M., and Goddard, P. 1996. Biology and distribution of arrowtooth, *Atheresthes stomias*, and Kamchatka, *A. evermanni*, flounders in Alaskan waters. Fish. Bull. **94**(2): 358–370.

Zuur, A.F., Ieno, E.N., Walker, N.J., Saveliev, A.A., and Smith, G.M. 2009. Mixed effects models and extensions in ecology with R. Springer Science+Business Media, LLC, New York.